Coupled Pore Relative Humidity Model for Concrete Shrinkage and Creep

Brock D. Hedegaard, Ph.D., P.E.[1], Timothy J. Clement[2], Mija H. Hubler, Ph.D.[3]

Biographical Sketches

ACI Member **Brock D. Hedegaard** is an associate professor at the University of Minnesota Duluth. He received his BS from Montana State University, and his MS and PhD from the University of Minnesota. He is a member of ACI Committees 209 (Creep and Shrinkage), 342 (Evaluation of Concrete Bridges), 435 (Deflections), and 444 (Structural Health Monitoring). His research interests include time-dependent structural analysis, substructural identification for structural health monitoring, and multiscale modeling.

ACI Member **Timothy J. Clement** is a structural engineer for Cleveland Cliffs located out of Silver Bay, Minnesota. He received his BS and MS from the University of Minnesota Duluth. His research interest is time-dependent model calibration.

ACI Member **Mija. H. Hubler** is an assistant professor at the University of Colorado, Boulder. She received her BS from the University of Illinois, her MS from Cornell University, and her PhD from Northwestern University. She is chair of ACI Committee 209 (Creep and Shrinkage). Her research interests include creep and shrinkage of concrete, fracture mechanics, and the development of novel construction materials.

[1] Department of Civil Engineering, University of Minnesota Duluth, 1405 University Drive, Duluth, Minnesota 55812, United States of America. Email: bhedeg@d.umn.edu
[2] Cleveland Cliffs, Northshore Mining, Silver Bay, Minnesota 55614, United States of America. Email: Tim.Clement@clevelandcliffs.com
[3] Dept. of Civil, Environmental, and Architectural Engineering, University of Colorado, Boulder, Engineering Center ECOT 646, Boulder, Colorado, 80309, United States of America. Email: Mija.Hubler@colorado.edu

Abstract

A new semi-empirical concrete shrinkage and creep model, called the CPRH Model, is proposed and calibrated. The new model proposes a coupling between autogenous and drying shrinkage using a volume-average pore relative humidity and treats drying creep as an additional stress-dependent shrinkage, linking together all these phenomena. The proposed expressions are designed to facilitate traditional integral-type analysis, but also uniquely support rate-type calculations that can be leveraged by analysis software. Model calibration uses the Northwestern University (NU) database of creep and shrinkage tests to determine new model parameters. The proposed model uses minimal inputs that are often known or may be assumed by the design engineer. Comparison of the proposed model to historical time-dependent models indicates that the new model provides a superior fit over a wider range of inputs.

Keywords

Creep, shrinkage, time-dependent behavior

Introduction

Concrete exhibits the time-dependent behaviors of shrinkage and creep, which primarily affect structural serviceability but also play an important role in long-term stress redistribution in any structure with permanent loads. Shrinkage is the strain caused by changes in moisture and chemical reactions that take place within the cement. There are two types of shrinkage commonly included in design predictions: autogenous shrinkage and drying shrinkage. Chemical hydration consumes water, a process called self-desiccation, which drives autogenous shrinkage [1]. Drying shrinkage occurs when moisture leaves the system through diffusion, causing a reduction in volume. Creep is the increase of strain with time under sustained stress. There are, similarly, two types of creep: basic creep and drying creep. Basic creep occurs under sealed conditions, and drying creep is the additional creep caused by drying when a loaded specimen is exposed to the environment. Shrinkage and creep tests are conducted for either sealed or unsealed conditions. Sealed tests do not allow the exchange of moisture with the atmosphere, and therefore measure only autogenous shrinkage and basic creep. Unsealed tests allow for measurement of total shrinkage and total creep.

Many design models have been proposed to predict shrinkage and creep of concrete, including the historical ACI 209 model [2], the B4 model [3], the GL2000 model [4], and the 2010 *fib* Model Code provisions [5]. Several of these models, while functional, have not been calibrated with respect to modern concrete mixes and may have some theoretical flaws (for example, no separation of drying and autogenous shrinkage, and volume-to-surface ratio scaling ultimate creep and shrinkage values instead of creep and shrinkage rates). The goal of this paper is to present a new time-dependent design model for concrete that meets the twin objectives of simplicity in application and theoretical rigor. The new model has been calibrated with respect to the NU creep and shrinkage database [6].

The model proposed herein, called the Coupled Pore Relative Humidity (CPRH) Model, builds from a previous model form [7] that had not been calibrated for use as a design model. The CPRH Model contains some simplifications from the previous model to facilitate adoption into structural engineering practice, but also some new theoretical developments. The primary ways where these two models differ are as follows:

1. The CPRH model couples the phenomena of self-desiccation and drying into a single relative pore humidity loss used to predict total shrinkage, whereas [7] neglects any discussion of self-desiccation and autogenous shrinkage, examining only drying shrinkage. In a related manner, the CPRH model uses the relative pore humidity loss

directly in predicting drying creep as a sort of stress-dependent shrinkage, meaning a form of “drying creep” may also occur during sealed creep tests. This possibility is neglected in [7], where only unsealed tests may have drying and associated drying creep.

2. The CPRH model retains the solidification-type aging only for viscoelasticity, whereas [7] also includes solidification for viscous flow, drying creep, and drying shrinkage. This simplification ensures that all expressions for the CPRH are analytical and do not need to be numerically integrated.
3. The CPRH model uses the hyperbolic tangent (tanh) expression for drying, whereas [7] used the error function (erf). Both satisfy diffusion theory, but the hyperbolic tangent is arguably more familiar to practicing civil engineers.
4. The CPRH model adopts a traditional aging elastic modulus, whereas [7] used a nonaging instantaneous modulus. This change aligns the CPRH model with common structural design practice in defining a creep coefficient.
5. All parameters for the CPRH model have been calibrated with respect to the NU database, whereas [7] included only fits to individual high-quality datasets.

In adopting these changes, the CPRH Model uniquely facilitates both traditional time-dependent analysis techniques, such as the use of a creep coefficient or the age-adjusted effective modulus method [8], and modern rate-type analysis [9].

The final calibrated model is presented first for the convenience of those who wish to apply the method. Next, the theoretical justification of the model is given. Finally, the CPRH Model predictions are compared to the database entries and predictions from other time-dependent models. The model calibration and uncertainty quantification procedures, which leverage the concept of profile likelihood plots [10], will be presented in a follow-up manuscript.

Research Significance

Accurate prediction of concrete time-dependent behavior is essential for maintaining serviceable and safe structures. This is particularly important for creep-sensitive structures such as high-rise buildings [11,12], concrete box-girder bridges [13,14], and prestressed beams. Many time-dependent models are outdated with respect to the growing database of experimental evidence [6]. This includes the previous ACI-209 model [2], which has recently been discontinued by that committee.

CPRH Model

For those wishing to apply the CPRH Model for time-dependent analysis, the procedure and equations are summarized in this section. All equations are given in both SI units (MPa, mm, and °C) and English units (psi, in., and °F). Model development and calibration was performed in SI units followed by conversion to English units; there are minor differences between the two formulations due to unit conversions and rounding. Sample calculations for SI and English units are provided in Appendices A and B, respectively.

Required Model Inputs

The CPRH Model is intended for design office purposes, and therefore relies on inputs that are either known or may be assumed by the designer. The following inputs are necessary, with suggested values given if not known:

- Mean 28-day concrete strength f_{cm} (MPa or psi). If design strength f_c' is given, then $f_{cm} = f_c' + 8$ MPa or $f_{cm} = f_c' + 1160$ psi.

- Aggregate volume ratio g (unitless). May calculate from mix design, but if unknown and assuming a typical normal-weight concrete mix, then estimate based on strength: $g = 0.707 - f_{cm}/(1250 \text{ MPa})$ or $g = 0.707 - f_{cm}/(181300 \text{ psi})$.
- Cement type: normal hardening (Type I) or rapid hardening (Type III). If unknown, assume Type I. Cement type is only used to estimate strength gain with time; other cement types may be used given data or expressions for strength versus time.
- Curing temperature T_c (°C or °F). If unknown, assume T_c = 20°C = 68°F.
- Average ambient temperature T (°C or °F). If unknown, assume T = 20°C = 68°F.
- Average ambient relative humidity h_0 (unitless). Provided as a decimal between 0 and 1. Refer to available meteorological data.
- Volume-to-surface ratio V/S (mm or in.).
- Duration of curing t_c (days).
- Time of loading t_0 (days).
- Analysis time t (days).

Shrinkage Prediction Model

The shrinkage strain expression $\varepsilon_{sh}(t)$ predicts the autogenous shrinkage strain alone if the concrete is sealed, or the total shrinkage strain if the concrete is exposed to the atmosphere:

$$\varepsilon_{sh}(t) = -p_{sh}\Delta H(t) \tag{1}$$

The negative sign in Equation (1) implies a reduction in volume, and p_{sh} is the shrinkage coefficient equal to:

$$p_{sh} = \begin{cases} 0.080\left(f_{cm}\right)^{-0.5}\left(1-g\right)^{1.7} & \text{for } f_{cm} \text{ in MPa} \\ 0.963\left(f_{cm}\right)^{-0.5}\left(1-g\right)^{1.7} & \text{for } f_{cm} \text{ in psi} \end{cases} \tag{2}$$

The change in pore relative humidity ΔH is a coupled expression between self-desiccation ΔH_{au} and drying ΔH_{dry}:

$$\Delta H(t) = \Delta H_{au}(t) + \Delta H_{dry}(t, t_c) - \Delta H_{au}(t)\Delta H_{dry}(t, t_c) \tag{3}$$

The change in pore relative humidity due to self-desiccation is

$$\Delta H_{au}(t) = p_{au} \ln\left(\frac{t - t_v}{\beta_{au}} + 1\right) \tag{4}$$

where t_v = 0.25 days is the duration prior to self-desiccation; for $t < t_v$, pore relative humidity is assumed to be saturated, that is $\Delta H_{au} = 0$. Parameters p_{au} (unitless) and β_{au} (units of days) are functions of the mean 28-day concrete strength f_{cm}:

$$p_{au} = \begin{cases} 0.012 + \dfrac{f_{cm}}{5000} & \text{for } f_{cm} \text{ in MPa} \\ 0.012 + \dfrac{f_{cm}}{725000} & \text{for } f_{cm} \text{ in psi} \end{cases} \tag{5}$$

$$\beta_{au} = \begin{cases} 10^{\left[33(f_{cm})^{-0.5} - 4\right]} & \text{for } f_{cm} \text{ in MPa} \\ 10^{\left[400(f_{cm})^{-0.5} - 4\right]} & \text{for } f_{cm} \text{ in psi} \end{cases} \tag{6}$$

The change in pore relative humidity due to drying is

$$\Delta H_{dry}(t, t_c) = 0.5\left(1 - h_0^2\right)\tanh\left(\sqrt{\frac{t - t_c}{\tau_{dry}}}\right) \tag{7}$$

where h_0 is the ambient relative humidity and t_c is the age at which drying commences (i.e., the curing duration) in days. For $t < t_c$ or when predicting autogenous shrinkage alone, no drying has occurred, so $\Delta H_{dry} = 0$. The shrinkage half-time τ_{dry} (units of days) is

$$\tau_{dry} = \begin{cases} 0.08\left(k_s \dfrac{V}{S}\right)^2 & \text{for } \dfrac{V}{S} \text{ in mm} \\ 51.6\left(k_s \dfrac{V}{S}\right)^2 & \text{for } \dfrac{V}{S} \text{ in inches} \end{cases} \tag{8}$$

The shape factor k_s depends on the shape of the concrete member, and is equal to:

$$k_s = \begin{cases} 1.00 & \text{infinite slab} \\ 1.18 & \text{infinite cylinder} \\ 1.22 & \text{infinite square prism} \\ 1.28 & \text{sphere} \\ 1.40 & \text{cube} \end{cases} \tag{9}$$

Most solid rectangular beams can be adequately modeled using k_s approximately equal to 1.2, though box girder walls may be more closely approximated as slabs with k_s nearer to 1.0.

Swelling Prediction Model

The swelling strain ε_{sw} proposed herein is only applicable for concrete submerged in water. In this case, $\Delta H = 0$ and the swelling strain is

$$\varepsilon_{sw}(t) = p_{sw}(t - t_{sw})^{0.2} \tag{10}$$

where t_{sw} is the age at which swelling begins in days. The positive sign of Equation (10) implies an increase in volume. Insufficient data exist to evaluate how swelling varies based on V/S or even concrete strength. A good estimate of the database was achieved by setting the swelling coefficient as a constant: $p_{sw} = 40 \times 10^{-6}$.

Creep Prediction Model

The compliance function $J(t,t_0)$ at time t for a load applied at time t_0 and having units of MPa^{-1} or psi^{-1} is given by

$$J(t,t_0) = R_{LL}\left[\frac{1}{E_{ct0}} + R_T J_b(t,t_0) + J_d(t,t_0)\right] \tag{11}$$

The elastic modulus E_{ct0} at age of loading t_0 is computed based on the concrete strength f_{ct0} also at age of loading t_0:

$$f_{ct0} = f_{cm}\left(\frac{t_0}{a + bt_0}\right) \tag{12}$$

$$E_{ct0} = \begin{cases} 4734\sqrt{f_{ct0}} & \text{for } f_{ct0} \text{ and } E_{ct0} \text{ in MPa} \\ 57000\sqrt{f_{ct0}} & \text{for } f_{ct0} \text{ and } E_{ct0} \text{ in psi} \end{cases} \tag{13}$$

where constants *a* and *b* are cement type dependent:

- For Type I cement, $a = 4.00$ days, $b = 0.85$ (unitless)
- For Type III cement, $a = 2.30$ days, $b = 0.92$ (unitless)

Load adjustment factor R_{LL} accounts for nonlinear effects due to high levels of stress:

$$R_{LL} = \begin{cases} 1 & \text{for } \dfrac{\sigma}{f_{ct0}} \le 0.5 \\ \exp\left(\dfrac{\sigma}{f_{ct0}} - 0.5\right) & \text{for } \dfrac{\sigma}{f_{ct0}} > 0.5 \end{cases} \tag{14}$$

where σ is the applied stress. The temperature adjustment factor R_T is presented in the next section documenting temperature correction procedures.

The basic creep compliance $J_b(t,t_0)$ has units of MPa^{-1} or psi^{-1} and is defined as:

$$J_b(t,t_0) = p_v\left(1 + \frac{1}{Kt_0}\right)\ln\left(\frac{t-t_0}{\beta_{cr}} + 1\right) + \left(p_f - \frac{p_v}{Kt_0}\right)\ln\left(\frac{t}{t_0}\right) \tag{15}$$

$$p_v = \begin{cases} 12.5\times10^{-6}\left(f_{cm}\right)^{-0.7} \\ 2.81\times10^{-6}\left(f_{cm}\right)^{-0.7} \end{cases} \quad p_f = \begin{cases} 30.0\times10^{-6}\left(f_{cm}\right)^{-0.5} & \text{for } f_{cm} \text{ in MPa} \\ 2.50\times10^{-6}\left(f_{cm}\right)^{-0.5} & \text{for } f_{cm} \text{ in psi} \end{cases} \tag{16}$$

where p_v is the nonaging viscoelastic compliance constant (units of MPa^{-1} or psi^{-1}), p_f is a flow constant (units of MPa^{-1} or ksi^{-1}), and the two time parameters K and β_{cr} are

$$K = 0.25 \text{ days}^{-1} \quad \beta_{cr} = 0.01 \text{ days} \tag{17}$$

The drying creep compliance $J_d(t,t_0)$ has units of MPa^{-1} or psi^{-1} and is defined as:

$$J_d(t,t_0) = p_d\left[\Delta H(t) - \Delta H(t_0)\right] \tag{18}$$

$$p_d = \begin{cases} 0.023\left(f_{cm}\right)^{-0.9}(1-g)^{1.7} & \text{for } f_{cm} \text{ in MPa} \\ 0.014\left(f_{cm}\right)^{-0.9}(1-g)^{1.7} & \text{for } f_{cm} \text{ in psi} \end{cases} \tag{19}$$

where p_d is the drying creep compliance constant (units of MPa^{-1} or psi^{-1}), and ΔH is evaluated at times t and t_0 per Equation (3). Unique among creep models, the CPRH Model predicts "drying creep" even for tests performed on sealed concrete, because $\Delta H(t)$ contains both self-desiccation and drying to the atmosphere. For sealed conditions, $\Delta H_{dry} = 0$ but $\Delta H_{au} > 0$.

If a traditional creep coefficient formulation is desired, the creep coefficient ϕ is defined by the ratio of the creep strain to the initial strain and is equal to

$$\phi(t,t_0) = E_{ct0} J(t,t_0) - 1 \tag{20}$$

Calibration of the model was done for compliance $J(t,t_0)$, not the creep coefficient $\phi(t,t_0)$. Therefore, if using the creep coefficient, the provided expression for f_{ct0} and E_{ct0} in Equations (12) and (13) must be used. Using other expressions for modulus with the given creep coefficient will return incorrect creep predictions.

Adjustments for Temperature

If temperatures are typical room temperature conditions (i.e., $T_c = T = 20°C = 68°F$), or if temperature conditions are unknown and assumed to be standard conditions, then no adjustments need to be made to the described model. For constant temperatures other than these standard conditions, two unitless corrections factors R_c and R_T shall be used to adjust time variables:

$$R_c = \begin{cases} \exp\left[U\left(\dfrac{1}{293} - \dfrac{1}{T_c + 273}\right)\right] & \text{for } T_c \text{ in °C} \\ \exp\left[U\left(\dfrac{1}{528} - \dfrac{1}{T_c + 460}\right)\right] & \text{for } T_c \text{ in °}F \end{cases} \tag{21}$$

$$R_T = \begin{cases} \exp\left[U\left(\dfrac{1}{293} - \dfrac{1}{T + 273}\right)\right] & \text{for } T \text{ in °C} \\ \exp\left[U\left(\dfrac{1}{528} - \dfrac{1}{T + 460}\right)\right] & \text{for } T \text{ in °}F \end{cases} \tag{22}$$

where U = 2500 K (Kelvin in SI) or U = 4500°R (degrees Rankine in English) is an activation energy constant, T_c is the curing temperature, and T is the ambient temperature after curing. Note that for standard conditions $T_c = T$ = 20°C = 68°F, both $R_c = R_T = 1$.

In the previously described shrinkage, swelling, and creep equations, all three base time variables (t_c, t_0, and t) should be replaced with the temperature-adjusted time variables (t_{cT}, t_{0T}, and t_T) as given in Table 1. Factor R_T is also used to amplify the basic creep compliance in Equation (11). The expressions in Table 1 assume that both t and t_0 are greater than t_c, which is typically the case for design applications. If $t_0 < t_c$, then $t_{0T} = R_c t_0$, and if $t < t_c$, then $t_T = R_c t$.

Total Response

The total response is the summation of the shrinkage strain with the load-induced strain, accounting for temperature effects by using the time-adjusted variables. For a constant stress σ applied at time t_0, the total strain is

$$\varepsilon_{total}\left(t_T, t_{0T}\right) = \sigma J\left(t_T, t_{0T}\right) + \varepsilon_{sh}\left(t_T\right) \tag{23}$$

Alternatively, if using the creep coefficient formulation from Equation (20):

$$\varepsilon_{total}\left(t_T, t_{0T}\right) = \frac{\sigma}{E_{ct0}}\left[1 + \phi\left(t_T, t_{0T}\right)\right] + \varepsilon_{sh}\left(t_T\right) \tag{24}$$

where $\varepsilon_{el} = \sigma / E_{ct0}$ is the elastic strain and $\varepsilon_{cr} = \sigma\phi(t_T, t_{0T})/E_{ct0}$ is the creep strain.

Assuming linear viscoelasticity for creep strains, the total strain under time-varying stress $\sigma(t)$ is given by the Boltzmann superposition principle:

$$\varepsilon_{total}\left(t_T\right) = \int_0^{t_T} J\left(t_T, \tau_{0T}\right) \frac{d\sigma\left(\tau_{0T}\right)}{d\tau_{0T}} d\tau_{0T} + \varepsilon_{sh}\left(t_T\right) \tag{25}$$

where τ_{0T} is the dummy time variable representing t_{0T} in the integration. Linear superposition is not applicable if $R_{LL} > 1$, meaning Equation (25) is intended only for sustained stresses less than half the concrete strength.

In any case, if the concrete is underwater, the shrinkage strain ε_{sh} should be replaced by the swelling strain ε_{sw} given by Equation (10).

Justification of Model Form

Self-Desiccation

The expression describing the change in pore relative humidity for sealed concrete, given in Equation (4), was fit to the four data curves collected by Jiang et al. [15] by adjusting parameters p_{au} and β_{au}; see Figure 1. Compressive strength values were not reported in the reference, so assumed values for strength were estimated from typical mix designs found in the NU shrinkage database. Table 2 presents the assumed compressive strength and the best fit values for p_{au} and β_{au} for each of the reported mixes. The duration of the water vapor saturation stage, given by t_v, is the time required to consume excess water and begin self-desiccation [16]. The value of t_v likely varies by the water-to-cement (w/c) ratio, as evidenced by the initial swelling period of low-strength concretes during autogenous shrinkage tests [17,18]. However, fits to the available data were not sensitive to the selection of t_v, so a constant value $t_v = 0.25$ days was assumed for simplicity. Nearly equivalent fits may be achieved by setting $t_v = \beta_{au} +$ 0.25 days.

For a design model, relationships for p_{au} and β_{au} based on mean compressive strength f_{cm} were desired. The relationships from Equations (5) and (6) provide predictions of self-desiccation within expected bounds for concretes with strength f_{cm} ranging from 20 to 100 MPa (2,900 to 14,500 psi); see Figure 2.

Drying

Drying shrinkage depends on diffusion of water through the concrete and exchange of this water with the atmosphere. Two fundamental functions for $\Delta H_{dry}(t,t_c)$ may be used to satisfy the requirements of diffusion theory [19] : the hyperbolic tangent function (tanh) and the error function (erf). The proposed model adopts the hyperbolic tangent function, as its use has already been established in the structural engineering community through previous models such as B4 [3]. The change in pore relative humidity due to drying alone $\Delta H_{dry}(t,t_c)$ is

$$\Delta H_{dry}\left(t,t_c\right) = -k_h \tanh\left(\sqrt{\frac{t-t_c}{\tau_{dry}}}\right) \tag{26}$$

where k_h is the drying coefficient that depends on the ambient relative humidity h_0 of the surrounding environment, and τ_{dry} is the characteristic drying time.

The diffusivity of concrete drops rapidly as pore relative humidity drops [20,21]. This nonlinearity has traditionally been captured by using a cubic [3,5] or quartic function [4] for the drying coefficient. However, these historical expressions for k_h appear to assume that the self-desiccation is negligible; see, for example, the justification of models B3 [22] and GL2000 [4].

Few references within the NU shrinkage database contain tests of the same concrete at multiple values of ambient relative humidity, with most tests being conducted at h_0 = 50% or 60%; see Figure 3. Keeton [23] tested concrete with w/c = 0.46, and the total shrinkage scales almost exactly to $(1–h_0^3)$; however, these data may have considerable autogenous shrinkage. Total shrinkage tests from Troxel et al. [24] on concrete with w/c = 0.59, assumed to have negligible autogenous shrinkage, and drying shrinkage tests from Pentala and Rautanen [25] both scale by $(1–h_0^2)$. Therefore for the proposed model, the adopted drying coefficient is

$$k_h = 0.5\left(1-h_0^{\,2}\right) \tag{27}$$

The inclusion of the 0.5 factor in Equation (27) assures that the adopted drying coefficient is always less than a linear function that would be applicable given linear diffusion;

see Figure 4. A function above this line would imply that the volume-averaged pore relative humidity could drop below the ambient humidity under drying only.

The characteristic drying time τ_{dry} (units of days) must be proportional to $(V/S)^2$ [19]:

$$\tau_{dry} = \tau_0 \left(k_s \frac{V}{S} \right)^2 \tag{28}$$

where τ_0 is a proportionality coefficient determined by calibration to the NU shrinkage database, and k_s is a shape factor accounting for the geometry of the cross section. Bažant et al. [26] originally proposed shape factors according to nonlinear drying computations [27]. However, more recent nonlinear diffusion finite element simulations [28] return different shape factors that depend on the ambient relative humidity. The values chosen for the CPRH model, given in Equation (9), are from these latest simulations [28] at h_0 = 60%, as this represents the most common testing condition in the database and a middling value for the k_s parameter.

Coupled Pore Relative Humidity

Self-desiccation and drying are coupled [21]. Self-desiccation in a sealed sample is uniform throughout the volume. However, in a drying specimen, self-desiccation is greater near the center and less near the surface, while drying is greater near the surface and less in the center. Furthermore, the rate of hydration that drives self-desiccation decreases as water is consumed.

This proposed model accomplishes the coupling with a “union” rule similar to computing the probability of the union of two events:

$$\Delta H(t) = \Delta H_{au}(t) + \Delta H_{dry}(t, t_c) - \Delta H_{au}(t) \Delta H_{dry}(t, t_c) \tag{29}$$

From this form, it is clear $\Delta H \leq 1$ unless either $\Delta H_{dry} > 1$ or $\Delta H_{au} > 1$. The logarithmic functional form of ΔH_{au} potentially violates this at very late ages for high-strength concrete. However, using the proposed expressions for self-desiccation, ΔH_{au} for f_{cm} = 167 MPa (which is the greatest measured strength found within the database) will not exceed one until after about one million years, which is well beyond the prediction horizon for the model.

Shrinkage Model

Historically, shrinkage design models have modeled either only the total shrinkage [2,4,22] or a summation of autogenous shrinkage and drying shrinkage [3,5]. In the proposed model, self-desiccation and drying mechanisms are combined by assuming the shrinkage strain is proportional to the change in pore relative humidity ΔH.

Shrinkage is roughly proportional to the elastic compliance [29]. Furthermore, because cement paste drives shrinkage and the aggregate does not change volume, the aggregate restrains and reduces the shrinkage. This aggregate effect can be considered using the Pickett relationship [30,31,32]. Considering strength and aggregate content together, the shrinkage coefficient is

$$p_{sh} = P_{sh}\left(f_{cm}\right)^{-r_{sh}}\left(1-g\right)^{r_g} \tag{30}$$

where P_{sh} is a unitless fitting coefficient, and r_{sh} and r_g are exponents. Values for P_{sh} and r_{sh} were calibrated to the autogenous and total shrinkage tests, together, from the NU database [6]. The calibrated value r_{sh} = 0.5 is consistent with the observations of Bažant and Li [29]. The value of r_g was set equal to 1.7, as previous studies [1,31,32] have consistently shown that this provides a serviceable fit for shrinkage.

If the aggregate content g is known from mix proportions, then its value may be used. In the common case that g is unknown, it may be approximated using

$$g = \begin{cases} 0.707 - \dfrac{f_{cm}}{1250} & \text{for } f_{cm} \text{ in MPa} \\ 0.707 - \dfrac{f_{cm}}{181300} & \text{for } f_{cm} \text{ in psi} \end{cases} \tag{31}$$

This expression for g was determined using all mixes in the NU database for which the measured value of 28-day concrete strength f_{cm} was given, mix values w/c, a/c, and c were all given, and aggregate was not specified as some form of lightweight aggregate. For this subset of mixes, g was estimated assuming that the aggregate density was equal to 2643 kg/m^3 (165 pcf) and the concrete density was 2323 kg/m^3 (145 pcf). Using these computed values of g, linear regression was performed using f_{cm} as the regressor, resulting in the above equations. Note that these expressions are only intended for typical normal-weight concrete mixes.

Creep Model

Per solidification theory [33], an aging viscoelastic compliance $J(t,t_0)$ at time t for load applied at time t_0 may be derived from a nonaging creep function $C(t–t_0)$ of precipitated material, a volume growth function $v(t)$ that represents the rate of precipitation, and a time-dependent viscosity $\eta(t)$ for viscous flow. The aging basic creep compliance rate is given by:

$$\dot{J}\left(t,t_0\right)=\frac{\dot{C}\left(t-t_0\right)}{v(t)}+\frac{1}{\eta\left(t\right)} \tag{32}$$

where the overdot represents the derivative with respect to time t. This compliance rate equation facilitates the use of rate-type analysis techniques.

The chosen form of the nonaging creep function is

$$C\left(t-t_0\right)=p_v\ln\left(\frac{t-t_0}{\beta_{cr}}+1\right) \tag{33}$$

where p_v is the nonaging viscoelastic compliance constant (units of MPa^{-1} or psi^{-1}), and β_{cr} is a time constant (units of days). The nonaging creep rate is therefore

$$\dot{C}\left(t-t_0\right)=\frac{p_v}{t-t_0+\beta_{cr}} \tag{34}$$

Nanoindentation tests on calcium-silicate-hydrate (C-S-H) [34] indicate that β_{cr} is on the order of 1.6 seconds. This implies significant creep occurs within seconds after loading, justifying the adoption of a nonaging instantaneous compliance [3,7]. However, the industry panel advising the development of this model indicated that a traditional aging modulus formulation was more familiar to most practitioners, who already use this so-called "elastic" modulus to compute short-term deflections. Concrete modulus testing uses slow loading rates applied over several minutes, and therefore some creep is factored into the traditional expressions for elastic modulus. To avoid double counting short-term creep, the value of β_{cr} = 0.01 days was selected. For data points measured less than 0.01 days after loading, this increase in β_{cr} affects the fit. However, because of uncertainty in creep test loading rates and inconsistent reporting of initial deformations [35], these short-term data points have significant uncertainty.

The volume growth function is inspired by a form similar to the time-dependent concrete strength gain as presented in ACI 209.R-92 [2,7]:

$$v(t) = \frac{Kt}{Kt+1} \tag{35}$$

where K is a rate constant (units of days^{-1}) calibrated using the NU creep database.

The viscosity is assumed to increase linearly with time:

$$\eta(t) = \frac{t}{p_f} \tag{36}$$

where p_f is a flow constant (units of MPa^{-1} or ksi^{-1}). This expression for the aging viscosity is consistent with the B4 model, which is justified by microprestress theory [36].

Substituting Equations (34) through (36) into Equation (32) yields the aging creep compliance rate:

$$\dot{J}(t,t_0) = \left(\frac{1}{Kt}+1\right)\left(\frac{p_v}{t-t_0+\beta_{cr}}\right)+\frac{p_f}{t} \tag{37}$$

The creep compliance function arises by taking the integral:

$$J(t,t_0) = \int_{t_0}^{t} \dot{J}(\tau,t_0)\,d\tau = \frac{1}{E_{ct0}} + \frac{p_v}{K}\left(\frac{1}{t_0-\beta_{cr}}\right)\ln\left(\frac{t_0}{t}\left(\frac{t-t_0}{\beta_{cr}}+1\right)\right) + p_v\ln\left(\frac{t-t_0}{\beta_{cr}}+1\right) + p_f\ln\left(\frac{t}{t_0}\right) \tag{38}$$

where E_{ct0} is the elastic modulus at age of loading t_0. For $t_0 >> \beta_{cr}$, which is true so long as the concrete is at least several hours old prior to loading, then this expression may be simplified to the elastic compliance plus the basic creep terms expressed in Equation (17):

$$J(t,t_0) = \frac{1}{E_{ct0}} + p_v\left(1+\frac{1}{Kt_0}\right)\ln\left(\frac{t-t_0}{\beta}+1\right) + \left(p_f - \frac{p_v}{Kt_0}\right)\ln\left(\frac{t}{t_0}\right) \tag{39}$$

The two basic creep parameters p_v and p_f were proposed as functions of mean concrete strength f_{cm}:

$$p_v = P_v\left(f_{cm}\right)^{-r_v} \tag{40}$$

$$p_f = P_f\left(f_{cm}\right)^{-r_f} \tag{41}$$

where P_v and P_f are fitting coefficients with units of MPa^{-1} or psi^{-1}, and r_v and r_f are exponents. Values for P_v, P_f, r_v, and r_f were calibrated to the NU creep database.

The “drying creep” in the CPRH Model is better described as load-induced shrinkage [37] because it shares the functional form of the shrinkage model and is driven by both self-desiccation and drying. Furthermore, this drying creep formulation ensures that pre-dried specimens have reduced compliance during both basic creep tests and total creep tests [38,39]. In rate-type analysis, drying creep may be combined into the shrinkage rate $\dot{\varepsilon}_{sh}$:

$$\dot{\varepsilon}_{sh} = \left(-p_{sh} + \sigma p_d\right)\Delta\dot{H} \tag{42}$$

where $\Delta\dot{H}$ is the rate of change of pore relative humidity.

Because of the analogous nature of drying creep and shrinkage, the proposed drying creep parameter p_d shares the same form as the shrinkage coefficient:

$$p_d = P_d \left(f_{cm} \right)^{-r_d} \left(1 - g \right)^{r_g} \tag{43}$$

where P_d is a fitting coefficient with units of MPa^{-1} or psi^{-1}, and r_d and r_g are exponents. Values for P_d and r_d were calibrated to the NU creep database, and the value of r_g was defined as equal to 1.7, as was done for shrinkage.

The terms for high stress levels R_{LL} and temperature R_c and R_T were adopted and modified from the *fib* Model Code 2010 [5] and the Arrhenius equation in model B4 [3], respectively. The Arrhenius equation models the increased likelihood that the activation energy for a reaction (curing time using R_c) or deformation (creep and shrinkage using R_T) will be exceeded at elevated temperatures due to the increased kinetic energy of the molecules. For phenomena that are limited by the quantity of some material, namely water for drying and reactants for hydration, only the rate and not the ultimate value is affected by the Arrhenius equation. This is, admittedly, a simplification that deserves further investigation. For example, concrete is unlikely to ever be "fully dried" under ambient conditions, and the amount of water available for drying could theoretically increase with increased temperature. For basic creep, which is not strictly limited by some material quantity, both the rate and magnitude are adjusted using R_T; see Equation (11). The rate increase reflects the increased likelihood that any one creep site may "slip" under higher temperature, and the magnitude increase reflects the greater number of available creep sites that may slip at this temperature.

Comparison to Database and Historical Models

The NU creep and shrinkage database [6] version obtained on December 9, 2019, was used to calibrate the CPRH Model parameters. This version of the NU database contained approximately 1884 shrinkage tests and 1439 creep tests. Some entries in the database were improperly or incompletely reported. Datasets that could not be corrected using original sources were discarded (that is, “blacklisted”) so they did not adversely affect the fit. Furthermore, datasets were blacklisted if the material or testing conditions were not of interest for the final model, such as tests on cement paste and creep tests with variable loading. After blacklisting, 1342 shrinkage tests (787 with admixtures) and 923 creep tests (527 with admixtures) remained.

Figures 5 and 6 show the properties of the tests in the shrinkage and creep databases, respectively, after blacklisting. N-values indicate the numbers of tests where the parameter is given in the database. The database contains w/c ratios primarily between 0.2 and 0.8. Measured concrete strengths f_{cm} vary mainly between 20 MPa (3,000 psi) and 120 MPa (17,000 psi). Most specimens are 100-mm (4-in.) diameter cylinders or 100-mm (4-in.) sided prisms with V/S = 25 mm (1.0 in.), or 150-mm (6-in.) cylinders with V/S = 37.5 mm (1.5 in.). Cement type was given in the database as R = regular, RS = rapid set, or SL = slow hardening. The database contains many international tests, and international standards and designations for cement types are not always consistent. However, R, RS, and SL roughly map to Type I, Type III, and Type II cements, respectively, per ASTM classification.

The calibrated CPRH Model was compared to the remaining 1342 shrinkage tests and 923 creep tests by plotting the predicted versus measured shrinkage and swelling in Figure 7 and the predicted versus measured compliance in Figure 8. Shrinkage and creep exhibit significant scatter, so these plots primarily serve to highlight any systemic biases or skews in the model. Overall, the model appears to underestimate autogenous shrinkage. Autogenous shrinkage does not have an established, consistent test protocol throughout the database, and many tests in the autogenous shrinkage database have very rapid strain at early ages; it is unclear if some of these tests contain plastic shrinkage. Drying shrinkage predictions equal the difference between a total shrinkage prediction ($\Delta H_{dry} > 0$) and an autogenous shrinkage prediction ($\Delta H_{dry} = 0$). The coupled nature of the model does not result in a monotonic drying shrinkage prediction, so comparisons to drying shrinkage data may be incompatible. Total shrinkage, basic creep, and total creep plots appear to minimize skew in the predictions.

A weighted coefficient of variation of prediction errors [29] was used to quantify the goodness of fit. First, weights were assigned to all measurements y_i for $i = 1$ to N, where N is the total number of data points considered. Weighting ensured that the coefficient of variation represented the goodness of fit for all test durations, not just short duration tests that contained the majority of the data points in the database. Logarithmic time intervals (i.e., bins) were defined for t–t_c for shrinkage and t–t_0 for creep using powers of 4, such that Bin 1 was from 0 to 4 days, Bin 2 was from 4 to 16 days, Bin 3 was from 16 to 64 days, and so on. Each bin was given equal weight, and furthermore all tests within each bin were given equal weight regardless of their different data sampling rates. To achieve this, let n_{jk} be the number of data points from test j located in bin k, and let m_k be the number of tests that contain at least one point in bin k. The raw weight W_i of each data point i from test j and located in bin k is given by:

$$W_i = \frac{1}{n_{jk} m_k} \tag{44}$$

The normalized weights w_i were then calculated such that the summation of w_i for all points $i = 1$ to N is equal to 1:

$$w_i = \frac{W_i}{\sum_{\hat{i}=1}^{N} W_{\hat{i}}} \tag{45}$$

Using the normalized weights, the standard error s of the prediction model is defined as:

$$s=\sqrt{\left(\frac{1}{1-\sum_{i=1}^{N}w_i^2}\right)\sum_{i=1}^{N}w_i\left(Y_i-y_i\right)^2} \tag{46}$$

where Y_i is the model prediction for point i. If all weights w_i are equal, the multiplier $1/(1–\Sigma w_i^2)$ is equal to $N/(N–1)$ used for typical unweighted sample statistics. The weighted coefficient of variation of prediction errors ω is given by:

$$\omega=\frac{s}{y_m} \tag{47}$$

where y_m is the weighted mean of the measurements

$$y_m=\sum_{i=1}^{N}w_i y_i \tag{48}$$

Weighted coefficients of variation of prediction errors were computed for different subsets of the database to ensure that the model was not biased toward specific material or testing conditions. Shrinkage model coefficients are summarized in Table 3, and compliance model coefficients are summarized in Table 4. The "All Datasets" filter contained the datasets used for model calibration with blacklisting as described above. The "B4 Limits" filter represents only the datasets that conform to the stated limits of applicability of the B4 model [3], which are typical of engineering practice. The CPRH Model overestimates total shrinkage and underestimates autogenous shrinkage for SL cement and for tests conducted at high temperatures. A simple reduction factor for shrinkage of SL cement, as is proposed by the GL2000 model [4], cannot address this; a rebalancing of the proportions of autogenous to drying shrinkage may be necessary for different cement types. By comparison, the creep model does not appear to have any strong biases, performing similarly for all subsets.

The CPRH Model was compared to other historical design office models: ACI 209 [2], GL2000 [4], *fib* Model Code 2010 [5], B4 and the strength-based B4s [3], and the same two B4 models with the recent autogenous shrinkage update [32], called B4a and B4sa in this manuscript. All computations using B4 or B4s were done without aggregate or admixture correction factors. Models were compared by computing the weighted coefficient of variation of prediction errors as described above using either the "All Datasets" filter used for the proposed model calibration or the narrower "B4 Limits" filter.

Shrinkage model comparisons are presented in Table 5. Autogenous shrinkage and drying shrinkage are not separated in ACI 209 and GL2000 models, nor do these models have expressions for swelling, and therefore these entries are omitted in Table 5. Overall, the CPRH Model fares the best among the design office models, though there is admittedly bias in this conclusion because no other model was calibrated to all the datasets in either filtered set. Even though it was calibrated on a much smaller dataset, the GL2000 model performs admirably. Models B4s and *fib* 2010 perform well with total shrinkage, but are comparatively poor with autogenous shrinkage. Model B4 improves dramatically when applied only to the "B4 Limits" datasets, but still does not outperform the B4s model. The autogenous shrinkage update [32] improves the total shrinkage estimate of B4s and greatly improves the autogenous shrinkage estimate of B4, making B4a the best model for predicting autogenous shrinkage alone. Interestingly, this update degrades the total shrinkage estimate of B4, indicating the need for a recalibration of the drying shrinkage terms in B4.

Creep model comparisons are presented in Table 6. ACI 209 only defines the total creep and does not explicitly separate basic and drying creep terms; in this case, the basic creep prediction was simply the total creep evaluated at $h_0 = 1$. Again, the CPRH Model has the best performance, followed by the GL2000 model. Model B4s exhibited unexpected behavior, particularly for high temperature tests (T > 50°C) or low-strength concrete (f_{cm} < 20 MPa). There may also be inconsistencies in the published drying creep parameters for this model, as these deviate significantly from the analogous B4 drying creep parameters. The B4 model is sensitive to inputs outside its calibrated range as indicated by the difference between the coefficients of variation of prediction errors computed using “All Datasets” versus “B4 Limits”.

The CPRH Model was compared to selected datasets from the database to illustrate the shape of the model time equations and to show how the model adapts to certain inputs. Chosen datasets are not necessarily those best fit by the model, but are quality datasets that vary a parameter of interest. The shrinkage and swelling models are compared to selected datasets [23,40,41,42] in Figure 9. The creep model is compared to selected datasets [40,43,24] in Figure 10. The plots indicate that, while the shrinkage or creep coefficients may not exactly fit the data for all datasets, the model can capture the effects of changing ambient humidity, *V/S* ratio, curing time, and loading age.

Conclusions

The proposed design-office shrinkage and creep model, called the CPRH Model, has several advantages over existing time-dependent models. The shrinkage model adopts an innovative premise, wherein shrinkage is proportional to changes in pore relative humidity. The model couples self-desiccation and drying, meaning autogenous shrinkage and drying shrinkage as traditionally defined are not strictly additive. Drying creep is similarly proportional to the applied load and the change in pore relative humidity and is therefore equivalent to stress-dependent shrinkage. This means that tests on sealed specimens, which have traditionally been assumed to have only basic creep, will have drying creep associated with self-desiccation per the proposed model. Thus, the model can capture reductions in creep seen in sealed creep tests of pre-dried concrete. The basic creep expression is derived from solidification theory, and therefore has a convenient rate form and does not suffer from divergence issues that many other historical models encounter. Altogether, the CPRH Model form facilitates both traditional (i.e., integral-type) time-dependent analysis using shrinkage and compliance functions or rate-type analysis using shrinkage and compliance rates.

Inputs are confined to parameters that are either known or may be assumed by the designer, even during preliminary design stages. The model fit has been compared to subsets of the NU database, showing that the model is applicable over a wide range of inputs, including concrete with mean 28-day strength up to 120 MPa (17,000 psi). Overall, the proposed shrinkage and creep models consistently have lower coefficients of variations than all peer historical models when compared to the NU database. The superiority of the proposed model predictions even holds when computing the coefficient of variation of prediction errors for the more limited dataset that conforms to the published limits of applicability of the B4 model [3].

Acknowledgements

We thank the Concrete Research Council of the ACI Foundation for their support of this project. We also thank our industry panelists for their feedback: Alessandro Beghini, SOM; Matthew D'Ambrosia, MJ2 Consulting; Chris Burgess and Mike Keller, FIGG; Cullen O'Neill, MBJ; Andy Foden and Michael Brown, WSP; and Todd Nelson, WJE. Finally, we acknowledge the support of ACI Committee 209 and our committee liaison, Roman Wan-Wendner.

References

1. Neville, A.M., (1964). "Creep of concrete as a function of its cement paste content." *Magazine of Concrete Research*, *16*(46), pp. 21-30.
2. ACI Committee 209 (1982). *ACI 209R-82 Prediction of Creep, Shrinkage, and Temperature Effects in Concrete Structures*. American Concrete Institute, Detroit, MI.

3. RILEM TC-242-MDC (2015). "RILEM draft recommendation: TC-242-MDC multi-decade creep and shrinkage of concrete: material model and structural analysis." *Materials and Structures*, Vol. 48, No. 4, pp. 753-770.
4. Gardner, N.J., and Lockman, M.J. (2001). "Design Provisions for Drying Shrinkage and Creep of Normal-Strength Concrete," *ACI Materials Journal*, Vol. 98, No. 2, pp. 159-167.
5. fédération internationale du béton (2013). fib *Model Code for Concrete Structures 2010*. Ernst and Sohn, Wiley, Berlin, Germany.
6. Hubler, M.H., Wendner, R., and Bažant, Z.P. (2015). "Comprehensive database for concrete creep and shrinkage: Analysis and recommendations for testing and recording." *ACI Materials Journal*, 112(4), pp. 547-558.
7. Hedegaard, B.D. (2020). "Creep and Shrinkage Modeling of Concrete using Solidification Theory," *Journal of Materials in Civil Engineering*, Vol. 32, No. 7, 04020179.
8. Bazant, Z.P. (1972). "Prediction of concrete creep effects using age-adjusted effective modulus method." *ACI Journal*, 69(4), pp.212-217.
9. Di Luzio, G., Cedolin, L. and Beltrami, C. (2020). "Tridimensional long-term finite element analysis of reinforced concrete structures with rate-type creep approach." *Applied Sciences*, 10(14), p.4772.
10. Eisenberg, M.C., and Jain, H.V. (2017). "A confidence building exercise in data and identifiability: Modeling cancer chemotherapy as a case study." *Journal of Theoretical Biology*, Vol. 431, pp. 63-78.
11. Carreira, D.J. and Poulos, T.D. (2007). "Designing for effects of creep and shrinkage in high-rise concrete buildings." *Special Publication*, 246, pp. 107-132.

12. Zou, D., Liu, T., Teng, J., Du, C. and Li, B. (2014). “Influence of creep and drying shrinkage of reinforced concrete shear walls on the axial shortening of high-rise buildings.” *Construction and Building Materials*, 55, pp. 46-56.
13. Bažant, Z.P., Yu, Q. and Li, G.H. (2012). “Excessive long-time deflections of prestressed box girders. I: Record-span bridge in Palau and other paradigms.” *Journal of structural engineering*, 138(6), pp. 676-686.
14. Hedegaard, B.D., French, C.E. and Shield, C.K. (2017). “Time-dependent monitoring and modeling of I-35W St. Anthony Falls Bridge. I: Analysis of monitoring data.” *Journal of Bridge Engineering*, 22(7), p. 04017025.
15. Jiang, Z., Sun, Z. and Wang, P. (2006). “Internal relative humidity distribution in high-performance cement paste due to moisture diffusion and self-desiccation.” *Cement and Concrete Research*, *36*(2), pp.320-325.
16. Ding, X., Zhang, J. and Wang, J. (2019). “Integrative modeling on self-desiccation and moisture diffusion in concrete based on variation of water content.” *Cement and Concrete Composites*, *97*, pp. 322-340.
17. Tazawa, E. and Miyazawa, S. (1993). “Autogeneous Shrinkage of Concrete and Its Importance in concrete technology,” *Creep and Shrinkage of Concrete, Proc. 5th Int'l. RILEM Symposium*, Barcelona, Spain, pp. 159-174.
18. Baroghel-Bouny, V., Mounanga, P., Khelidj, A., Loukili, A. and Rafaï, N. (2006). “Autogenous deformations of cement pastes: part II. W/C effects, micro–macro correlations, and threshold values.” *Cement and Concrete Research, 36*(1), pp.123-136.
19. Bažant, Z.P., and Kim, J.-K. (1991). “Consequences of diffusion theory for shrinkage of concrete.” *Materials and Structures*, Vol. 24, No. 5, pp. 323-326.

20. Zhang, J., Wang, J. and Gao, Y. (2016). “Moisture movement in early-age concrete under cement hydration and environmental drying.” *Magazine of Concrete Research*, *68*(8), pp. 391-408.

21. Rahimi-Aghdam, S., Rasoolinejad, M. and Bažant, Z.P. (2019). “Moisture diffusion in unsaturated self-desiccating concrete with humidity-dependent permeability and nonlinear sorption isotherm.” *Journal of Engineering Mechanics*, *145*(5), p.04019032.

22. Bažant, Z.P. and Baweja, S. (1995). “Creep and Shrinkage Prediction Equation for Analysis and Design of Concrete Structures – Model B3.” *Materials and Structures*, Vol. 28, pp. 357-365.

23. Keeton, J.R. (1965). “Study of creep in concrete, Technical reports R333-I, R333-II, R333-III," U.S. Naval civil engineering laboratory, Port Hueneme, California.

24. Troxel, G.E., Raphael, J.E. and Davis, R.W. (1958). “Long-time creep and shrinkage tests of plain and reinforced concrete,” *Proc. ASTM 58*, pp. 1101-1120.

25. Pentala, V. and Rautanen, T. (1990). “Microporosity, Creep and Shrinkage of High-Strength Concrete." *ACI SP 121-21*, 2nd International Symposium on High-Strength Concrete, edited by Weston T. Heston, pp. 409-432.

26. Bažant Z.P., Osman E., and Thonguthai, W. (1976). “Practical formulation of shrinkage and creep in concrete.” *Materials and Structures*, RILEM 9:395–406

27. Bažant, Z.P. and Najjar, L.J. (1972). “Nonlinear water diffusion in nonsaturated concrete.” *Matériaux et Construction*, *5*(1), pp.3-20.

28. Dönmez, A. and Bažant, Z.P., (2016). “Shape factors for concrete shrinkage and drying creep in model B4 refined by nonlinear diffusion analysis.” *Materials and Structures*, *49*(11), pp.4779-4784.

29. Bazant, Z.P. and Li, G.H., (2008). "Unbiased statistical comparison of creep and shrinkage prediction models." *ACI materials Journal*, *105*(6), pp.610-621.

30. Pickett, G., (1956). "Effect of aggregate on shrinkage of concrete and a hypothesis concerning shrinkage." *American Concrete Institute Journal*, *52*(1), pp. 581-590.

31. Grasley, Z.C., Lange, D.A., Brinks, A.J., D'Ambrosia, M.D. (2005). "Modeling autogenous shrinkage of concrete accounting for creep caused by aggregate restraint." In: *Proceedings of the 4th international seminar on self-desiccation and its importance in concrete technology*, NIST, Gaithersburg, MD, pp. 78–94.

32. Rasoolinejad, M., Rahimi-Aghdam, S. and Bažant, Z.P. (2019). "Prediction of autogenous shrinkage in concrete from material composition or strength calibrated by a large database, as update to model B4." *Materials and Structures*, *52*(2), pp. 1-17.

33. Bažant, Z.P., and Prasannan, S. (1989). "Solidification theory for concrete creep. I: Formulation," *Journal of Engineering Mechanics*, Vol. 115, No. 8, pp. 1691-1703.

34. Vandamme, M., and Ulm, F.-J. (2013). "Nanoindentation investigation of creep properties of calcium silicate hydrates." *Cement and Concrete Research*, Vol. 52, pp. 38-52.

35. Rasoolinejad, M., Rahimi-Aghdam, S. and Bažant, Z.P. (2018). "Statistical filtering of useful concrete creep data from imperfect laboratory tests." *Materials and Structures*, *51*(6), pp.1-14.

36. Bazant, Z.P., Hauggaard, A.B. and Baweja, S. (1997). "Microprestress-solidification theory for concrete creep. II: Algorithm and verification." *Journal of Engineering Mechanics*, Vol. 123, No. 11, pp. 1195-1201.

37. Bazant, Z.P. and Chern, J.C. (1985). "Concrete creep at variable humidity: constitutive law and mechanism." *Materials and structures*, Vol. 18, No. 1, pp. 1-20.

38. Acker, P. (1993). “Creep tests of concrete: why and how?”. In *Creep and Shrinkage of Concrete*, proceedings of the Fifth International RILEM Symposium, Barcelona, pp. 3-14.

39. Wesche, K., Schrage, I., and von Berg, W. (1978). “Versuche zum Einfluss des Belastungsalters auf das Kreicken von Beton,” *Deutscher Ausschuss fur Stahlbeton*, Vol. 295, pp. 68-156.

40. Theiner, Y., Drexel, M., Neuner, M., and Hofstetter, G. (2017). “Comprehensive study of concrete creep, shrinkage, and water content evolution under sealed and drying conditions.” *Strain*, *53*(2), p.e12223.

41. Wittmann, F.H., Bažant, Z.P., Alou, F., and Kim, J.K. (1987). “Statistics of shrinkage test data.” *Cement, Concrete, and Aggregates*, 9(2), pp.129-153.

42. Persson, B. (2002). “Eight-year exploration of shrinkage in high-performance concrete.” *Cement and Concrete Research*, 32(8), pp.1229-1237.

43. Komendant, G.J., Polivka, M., and Pirtz, D. (1976). “Study of concrete properties for prestressed concrete reactor vessels,” *Final Report No. UCSESM 76-3* (to General Atomic Company), Department of Civil Engineering, University of California, Berkeley.

Tables

Table 1. Temperature-adjusted time variables

Description	Base Time Variable	Adjusted Time Variable
Time of curing	t_c	$t_{cT} = R_c t_c$
Time of loading	t_0	$t_{0T} = t_{cT} + R_T(t_0 - t_c)$
Current time	t	$t_T = t_{cT} + R_T(t - t_c)$

Table 2. Self-desiccation fitting parameters and assumed mean 28-day strength [15]

w/c	Assumed f_{cm} (MPa)	p_{au}	β_{au} (days)
0.5	43	0.0200	8.30
0.4	57	0.0220	2.28
0.3	75	0.0245	0.65
0.2	99	0.0297	0.15

Table 3. Weighted coefficients of variation of prediction errors of proposed shrinkage model

Filter	**Weighted CoV of Prediction Errors**				
	Autogenous Shrinkage	Drying Shrinkage	Total Shrinkage	Swelling	**Autogenous and Total Shrinkage Combined**
All Datasets	0.69	0.43	0.36	0.72	**0.38**
Cement type = R	0.68	0.39	0.36	0.68	**0.38**
Cement type = RS	0.71	0.29	0.44	0.69	**0.47**
Cement type = SL	0.96	0.51	0.53	--	**0.55**
f_{cm} < 40 MPa	1.03	0.38	0.40	0.68	**0.40**
40 MPa ≤ f_{cm} < 80 MPa	0.88	0.45	0.32	0.83	**0.35**
f_{cm} ≥ 80 MPa	0.63	0.69	0.36	0.59	**0.45**
20°C ≤ T < 30°C	0.68	0.45	0.36	0.72	**0.38**
T ≥ 30°C	0.90	0.39	0.65	--	**0.83**
h_0 < 0.6	--	0.49	0.40	--	**--**
h_0 ≥ 0.6	--	0.43	0.30	--	**--**
B4 Limits	0.85	0.39	0.37	0.67	**0.38**

Table 4. Weighted coefficients of variation of prediction errors of proposed creep model

Filter	Weighted CoV of Prediction Errors		
	Basic Creep	Total Creep	**Basic and Total Creep Combined**
All Datasets	0.34	0.29	**0.31**
Cement type = R	0.38	0.33	**0.35**
Cement type = RS	0.32	0.19	**0.23**
Cement type = SL	0.28	0.26	**0.27**
f_{cm} < 40 MPa	0.35	0.26	**0.30**
40 MPa ≤ f_{cm} < 80 MPa	0.35	0.30	**0.31**
f_{cm} ≥ 80 MPa	0.31	0.30	**0.31**
20°C ≤ T < 30°C	0.33	0.28	**0.30**
T ≥ 30°C	0.41	0.39	**0.40**
$\sigma < 0.5f_{cm}$	0.36	0.28	**0.31**
$\sigma \geq 0.5f_{cm}$	0.27	0.31	**0.31**
B4 Limits	0.31	0.27	**0.29**

Table 5. Weighted coefficients of variation of historical shrinkage models for "All Datasets" filter | "B4 Limits" filter in NU database

Model	Coefficients of Variation				
	Autogenous Shrinkage	Drying Shrinkage	Total Shrinkage	Swelling	**Autogenous and Total Shrinkage Combined**
CPRH	0.69 | 0.85	0.43 | 0.39	0.36 | 0.37	0.72 | 0.67	**0.38 | 0.38**
ACI 209	--	--	0.47 | 0.46	--	--
GL2000	--	--	0.39 | 0.40	--	--
fib 2010	0.91 | 1.00	0.62 | 0.63	0.44 | 0.44	0.95 | 0.91	**0.48 | 0.46**
B4s	0.85 | 0.93	0.56 | 0.57	0.45 | 0.46	0.93 | 0.88	**0.48 | 0.47**
B4sa	0.90 | 0.77	0.56 | 0.57	0.42 | 0.40	0.93 | 0.88	**0.45 | 0.40**
B4	2.30 | 0.95	0.51 | 0.52	0.60 | 0.49	1.13 | 0.94	**0.76 | 0.50**
B4a	0.75 | 0.69	0.51 | 0.52	0.61 | 0.55	1.13 | 0.94	**0.62 | 0.56**

Table 6. Weighted coefficients of variation of historical creep models for "All Datasets" filter | "B4 Limits" filter in NU database

Model	**Coefficients of Variation**		
	Basic Creep	Total Creep	**Basic and Total Creep Combined**
CPRH	0.34 | 0.31	0.29 | 0.27	**0.31 | 0.29**
ACI 209	0.48 | 0.33	0.41 | 0.38	**0.44 | 0.37**
GL2000	0.44 | 0.31	0.35 | 0.31	**0.39 | 0.32**
fib 2010	0.49 | 0.35	0.41 | 0.39	**0.44 | 0.38**
B4s	12.03 | 1.28	1.33 | 0.81	**7.26 | 0.97**
B4	1.10 | 0.41	1.22 | 0.55	**1.18 | 0.52**

Figures

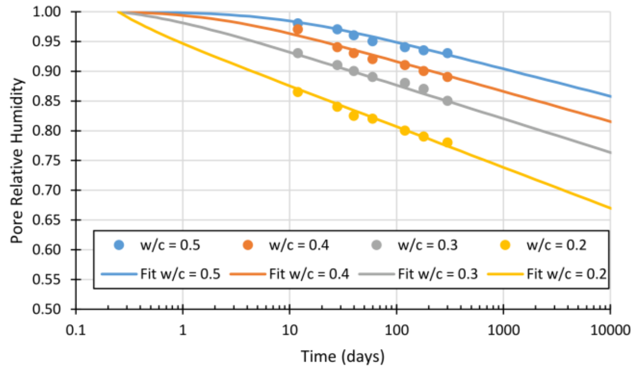

Figure 1. Pore relative humidity data under self-desiccation [15]

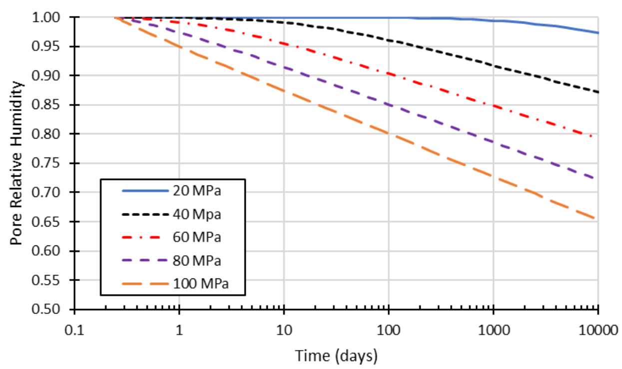

Figure 2. Proposed model for pore relative humidity under self-desiccation

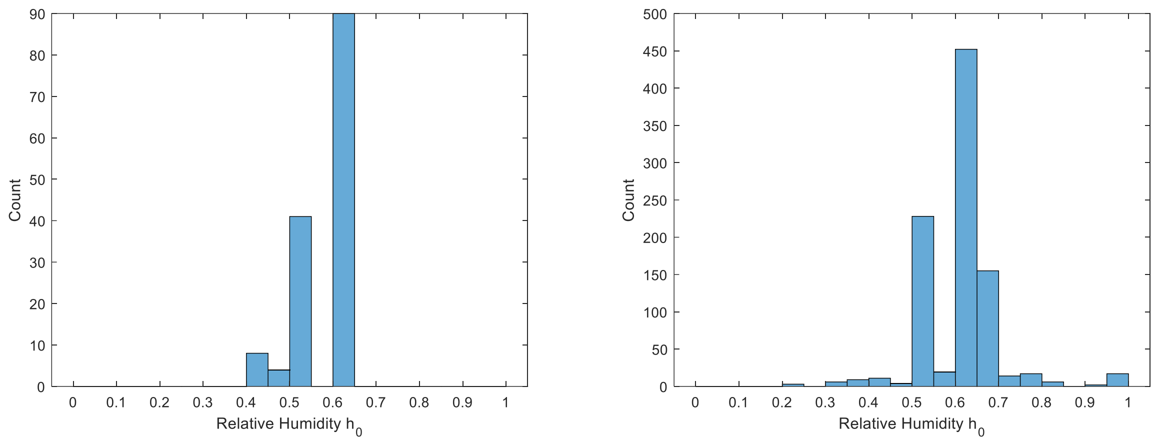

(a) Drying Shrinkage **(b) Total Shrinkage**

Figure 3. Distribution of ambient relative humidity *h*$_0$ for all (a) drying shrinkage and (b) total shrinkage tests used for model calibration

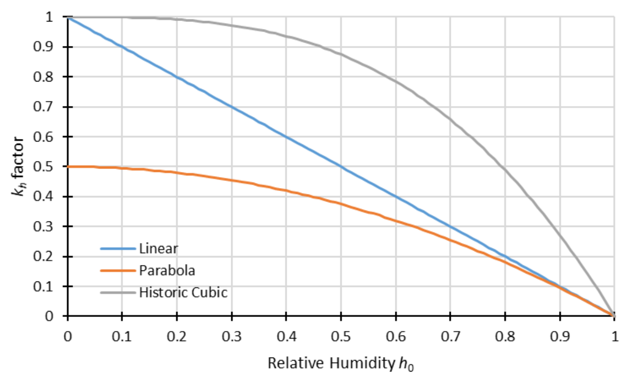

Figure 4. Comparison of drying coefficient *k*$_h$ forms

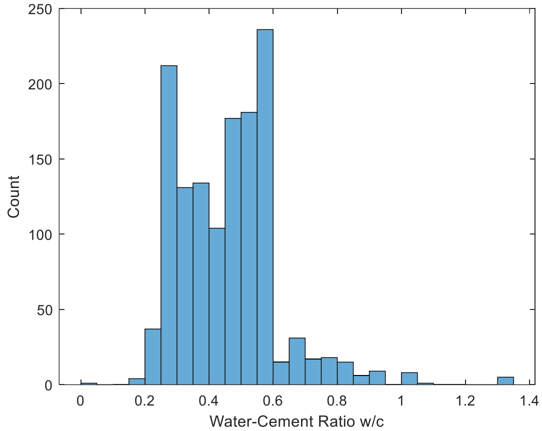

(a) *w/c* ratio (N = 1342)

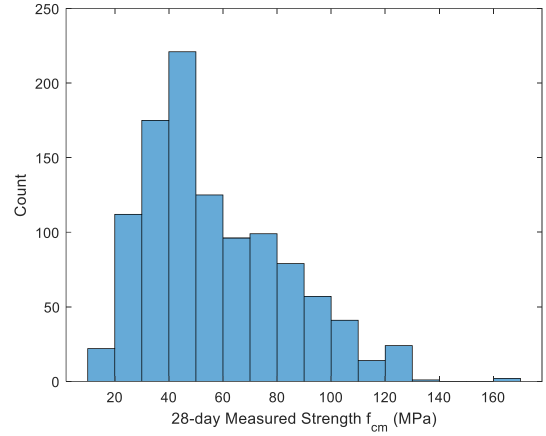

(b) Measured f_{cm} (N = 1068)

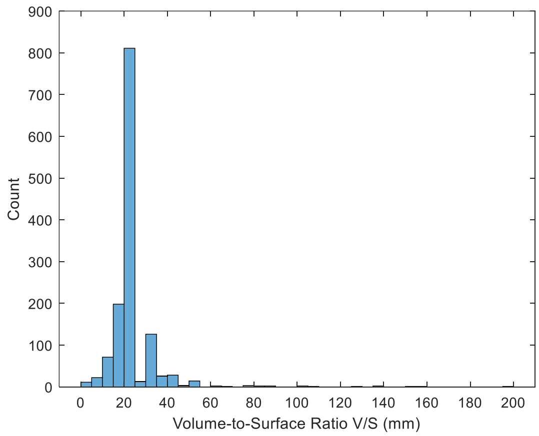

(c) *V/S* ratio (N = 1342)

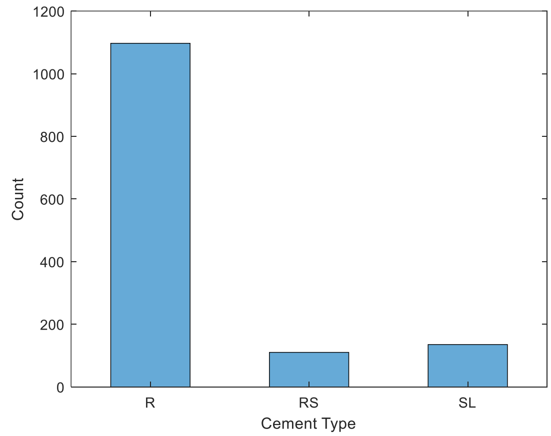

(d) Cement type (N = 1342)

Figure 5. Contents of shrinkage database used for model calibration

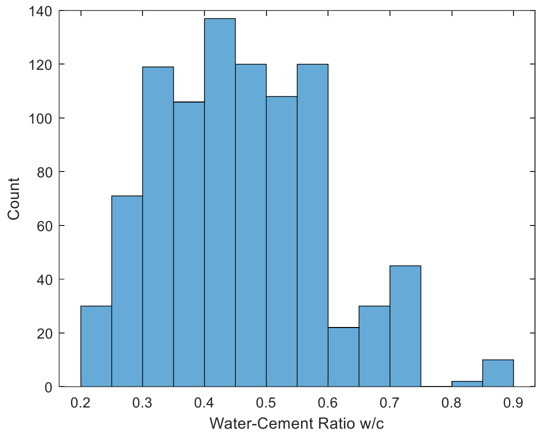

(a) w/c ratio (N = 920)

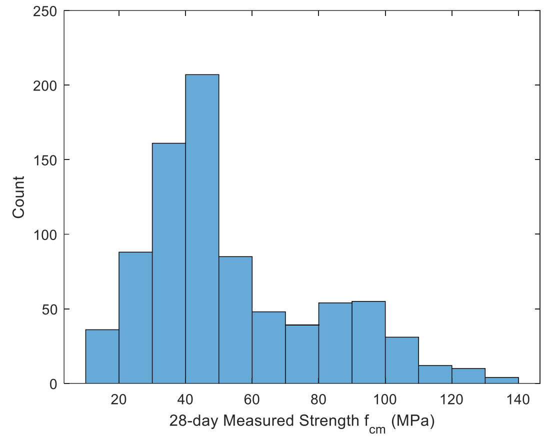

(b) Measured f_{cm} (N = 830)

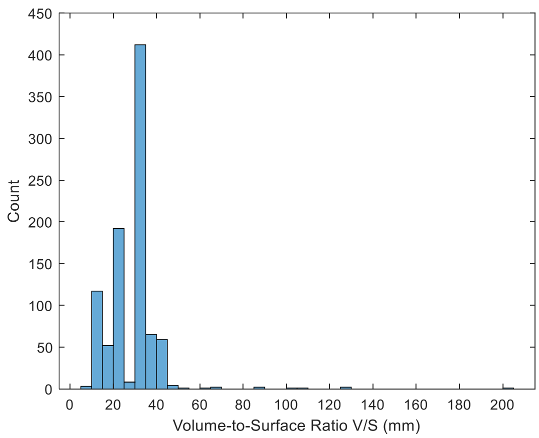

(c) V/S ratio (N = 923)

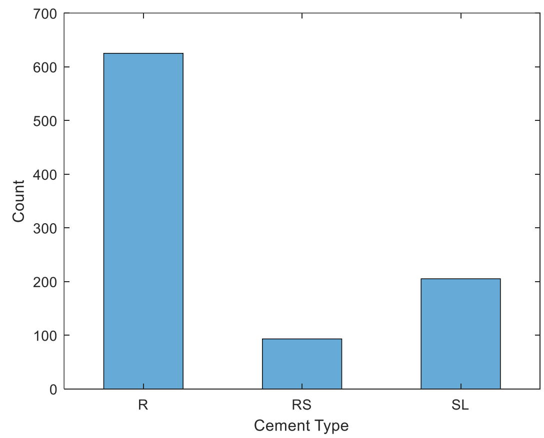

(d) Cement type (N = 923)

Figure 6. Contents of creep database used for model calibration

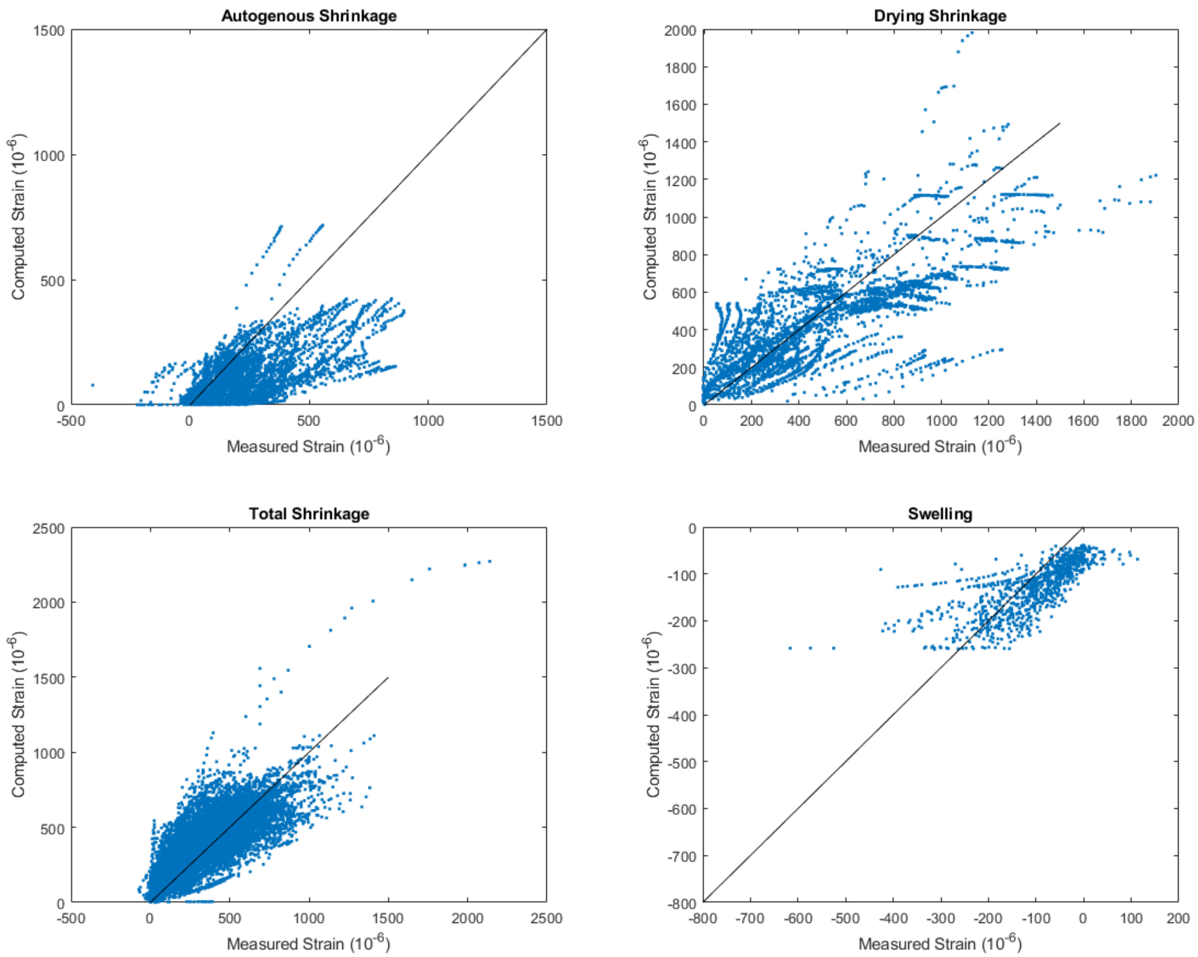

Figure 7. Predicted versus measured plots for proposed shrinkage and swelling models

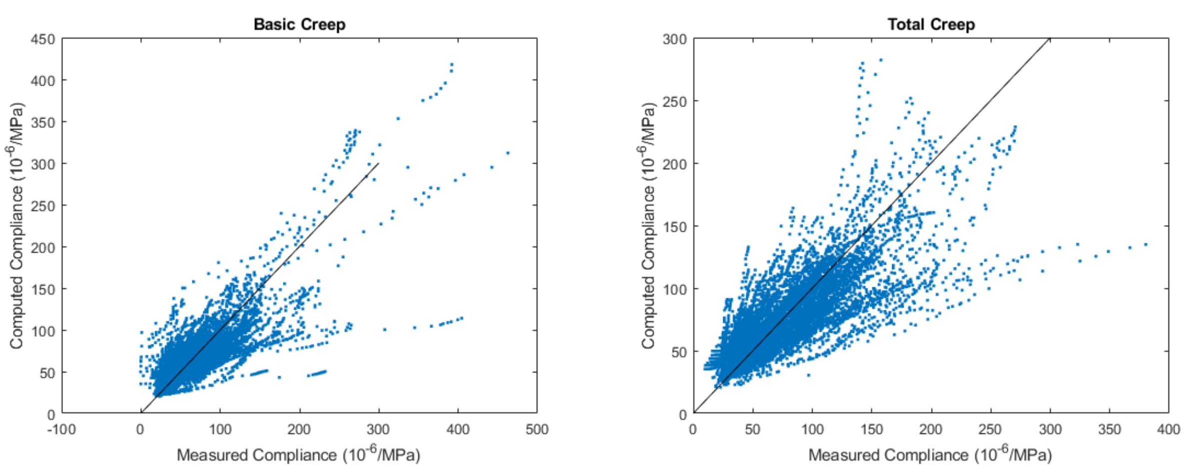

Figure 8. Predicted versus measured plots for proposed creep model

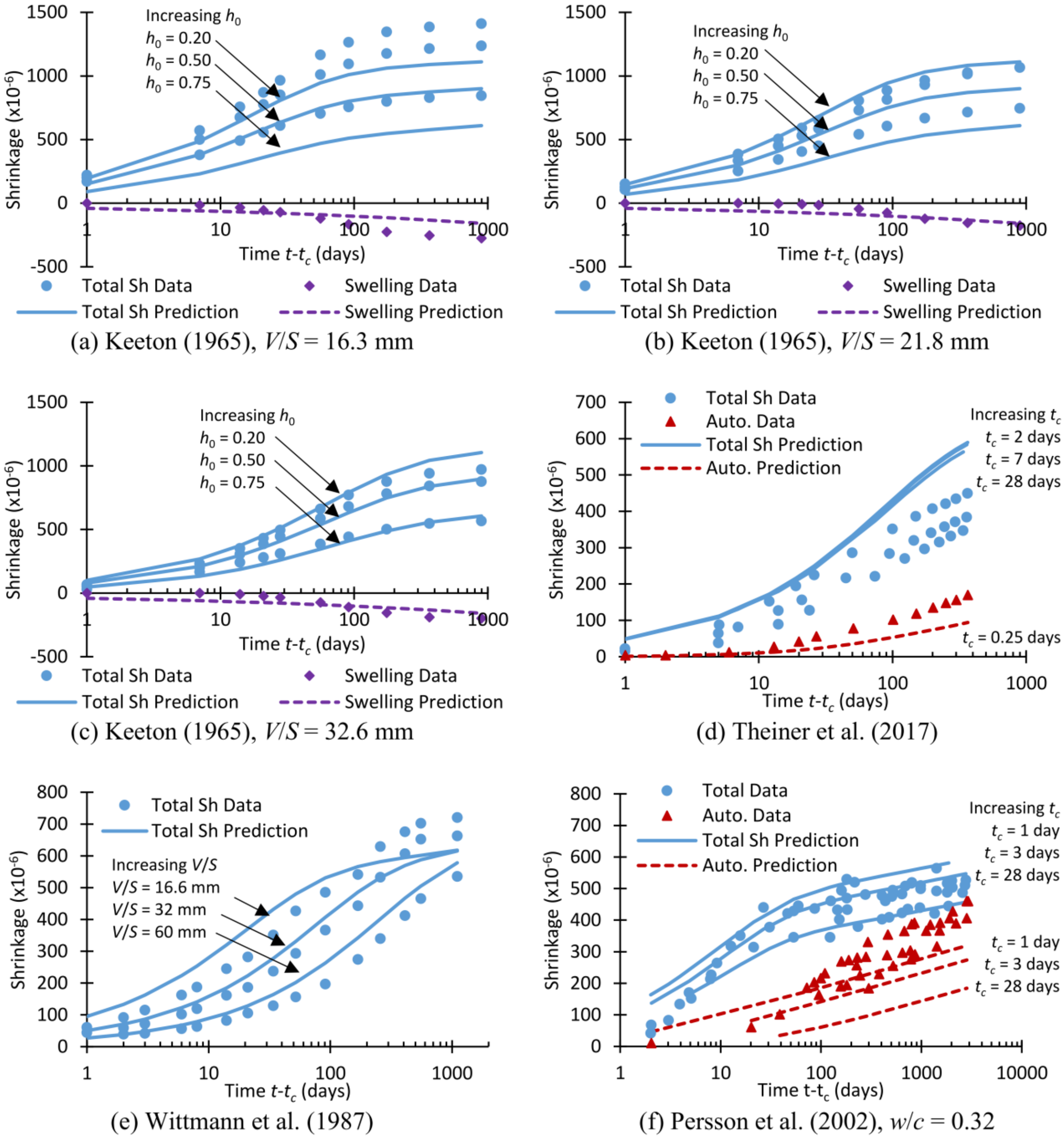

Figure 9. Proposed shrinkage model compared to selected datasets

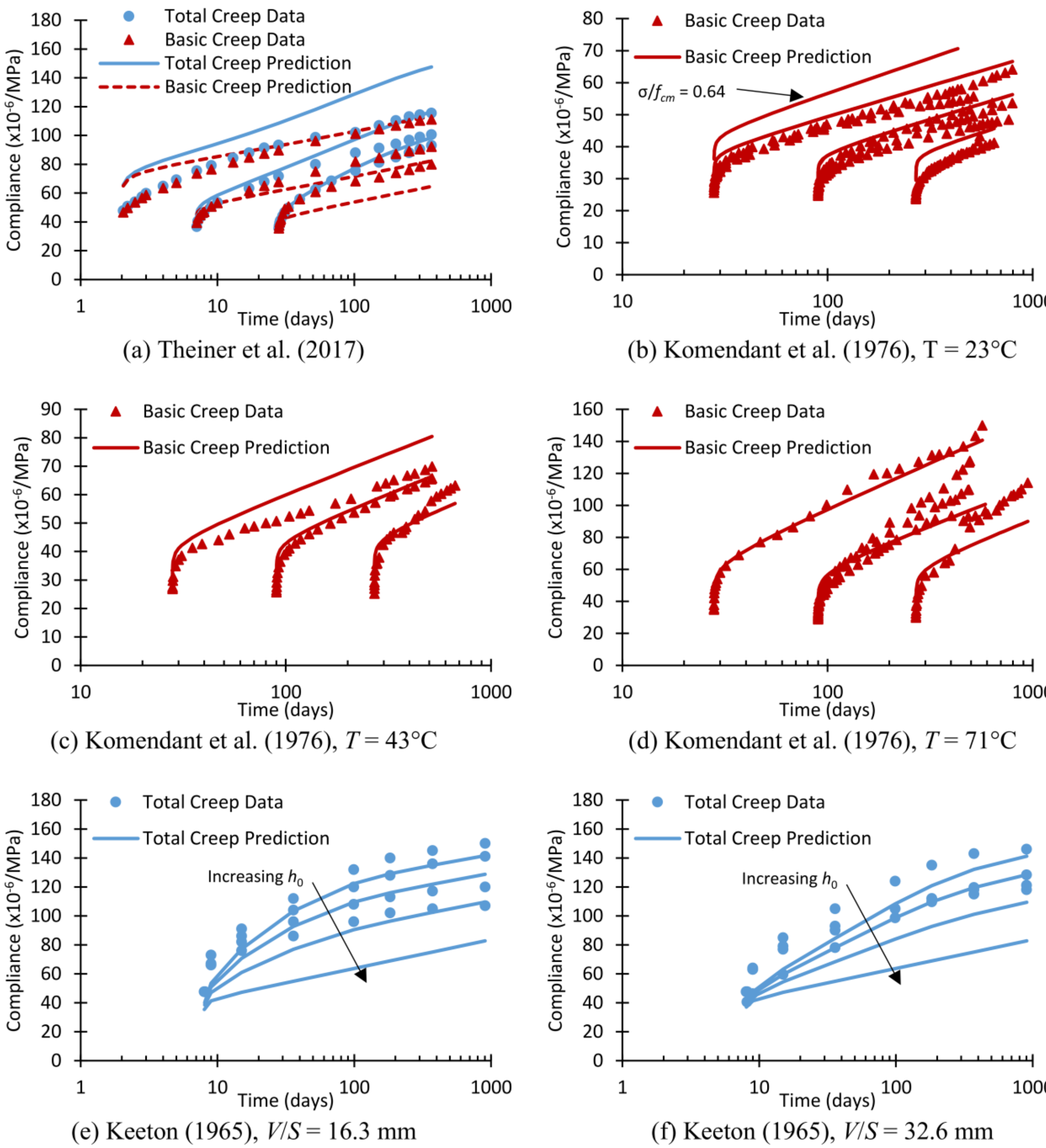

(a) Theiner et al. (2017)

(b) Komendant et al. (1976), T = 23°C

(c) Komendant et al. (1976), T = 43°C

(d) Komendant et al. (1976), T = 71°C

(e) Keeton (1965), V/S = 16.3 mm

(f) Keeton (1965), V/S = 32.6 mm

Figure 10. Proposed creep model compared to selected datasets

List of Tables

List of Figures

Appendix A: Example Calculations for SI Units

A 100-mm diameter cylinder is cured for t_c = 7 days at T_{cur} = 30°C, after which time it is allowed to dry subjected to T = 25°C and h_0 = 0.70 conditions. The cylinder is later loaded at 21 days with a sustained compressive stress of 6 MPa. The design 28-day strength of the cylinder f_c' = 40 MPa, and it is made from Type I cement. Other mix parameters are unknown.

Compute the time-dependent strains at t = 7 days, 21 days (just before and just after loading), 365 days, and 10,000 days.

Assumed Material Properties

Mean 28-day concrete strength f_{cm} and the aggregate volume fraction g are both unknown, and are therefore estimated from the design strength f_c' = 40 MPa:

$$f_{cm} = f_c' + 8 = 40 + 8 = 48 \text{ MPa} \tag{A-1}$$

$$g = 0.707 - \frac{f_{cm}}{1250} = 0.707 - \frac{48}{1250} = 0.6686 \tag{A-2}$$

Temperature Adjustments

Temperature is different from standard conditions, so temperature correction terms must be computed using U = 2500 Kelvin:

$$R_c = \exp\left[U\left(\frac{1}{293} - \frac{1}{T_{cur} + 273}\right)\right] = \exp\left[2500\left(\frac{1}{293} - \frac{1}{30 + 273}\right)\right] = 1.325 \tag{A-3}$$

$$R_T = \exp\left[U\left(\frac{1}{293} - \frac{1}{T + 273}\right)\right] = \exp\left[2500\left(\frac{1}{293} - \frac{1}{25 + 273}\right)\right] = 1.154 \tag{A-4}$$

These factors are used to adjust the curing time, time of loading, and analysis times:

$$t_{cT} = R_c t_c = 1.325(7) = 9.277 \text{ days} \tag{A-5}$$

$$t_{0T} = t_{cT} + R_T\left(t_0 - t_c\right) = 9.277 + 1.154(21 - 7) = 25.43 \text{ days} \tag{A-6}$$

$$t_T = t_{cT} + R_T\left(t - t_c\right) = 9.277 + 1.154\left(\begin{bmatrix}365\\10000\end{bmatrix} - 7\right) = \begin{bmatrix}422.4\\11540\end{bmatrix}\text{ days} \tag{A-7}$$

Shrinkage Calculations

The shrinkage coefficient p_{sh} is given by:

$$p_{sh} = 0.080\left(f_{cm}\right)^{-0.5}\left(1-g\right)^{1.7} = 0.080\left(48\right)^{-0.5}\left(1-0.6686\right)^{1.7} = 0.00177 \tag{A-8}$$

For self-desiccation, parameters p_{au} and β_{au} are given by:

$$p_{au} = 0.012 + \frac{f_{cm}}{5000} = 0.012 + \frac{48}{5000} = 0.0216 \tag{A-9}$$

$$\beta_{au} = 10^{\left(33\left(f_{cm}\right)^{-0.5}-4\right)} = 10^{\left(33\left(48\right)^{-0.5}-4\right)} = 5.80\text{ days} \tag{A-10}$$

The volume-to-surface ratio of a cylinder, assuming that the ends are not exposed to drying, is the area of a circle divided by the circumference of a circle, which equals half the radius. Therefore, a 100-mm diameter cylinder has V/S = 25 mm. Being a cylinder with sealed ends, shape factor k_s = 1.18 per Equation (9). These are used to compute the shrinkage half-time τ_{dry}:

$$\tau_{dry} = 0.08\left(k_s\frac{V}{S}\right)^2 = 0.08\left(1.18*25\right)^2 = 69.92\text{ days} \tag{A-11}$$

The change in pore relative humidity ΔH and resulting shrinkage strains ε_{sh} are computed at times t = 7, 21, 365, and 10,000 days. Detailed calculations are shown for t = 365 days, and the rest of the times are summarized in Table A-1.

$$\Delta H_{au}\left(t_T\right) = p_{au}\ln\left(\frac{t_T - t_v}{\beta_{au}} + 1\right) = 0.0216\ln\left(\frac{422.4-0.25}{5.80}+1\right) = 0.093 \tag{A-12}$$

$$\begin{aligned}\Delta H_{dry}\left(t_T, t_{cT}\right) &= 0.5\left(1-h_0{}^2\right)\tanh\left(\sqrt{\frac{t_T - t_{cT}}{\tau_{dry}}}\right)\\ &= 0.5\left(1-0.7^2\right)\tanh\left(\sqrt{\frac{422.4-9.277}{69.92}}\right) = 0.251\end{aligned} \tag{A-13}$$

$$\Delta H(t_T) = \Delta H_{au}(t_T) + \Delta H_{dry}(t_T, t_{cT}) - \Delta H_{au}(t_T)\Delta H_{dry}(t_T, t_{cT})$$
$$= 0.093 + 0.251 - 0.093 * 0.251 = 0.321 \quad \text{(A-14)}$$

$$\varepsilon_{sh}(t) = -p_{sh}\Delta H(t) = -0.00176 * 0.321 = -566 \times 10^{-6} \quad \text{(A-15)}$$

Table A-1: Results of Shrinkage Calculations

***t* (days)**	**t_T (days)**	**ΔH_{au}**	**ΔH_{dry}**	**ΔH**	**ε_{sh}**
7	9.277	0.020	0	0.020	-36×10^{-6}
21	25.43	0.036	0.114	0.146	-258×10^{-6}
365	422.4	0.096	0.251	0.321	-566×10^{-6}
10,000	11,540	0.164	0.255	0.377	-666×10^{-6}

Creep Calculations

First, the strength and modulus must be calculated at the time of loading. For Type I cement, $a = 4$ and $b = 0.85$, so the strength at $t_0 = 21$ days ($t_{0T} = 25.43$ days) is

$$f_{ct0} = f_{cm}\left(\frac{t_{0T}}{a + bt_{0T}}\right) = 48\left(\frac{25.43}{4 + 0.85 * 25.43}\right) = 47.65 \text{ MPa} \quad \text{(A-16)}$$

$$E_{ct0} = 4734\sqrt{f_{ct0}} = 4734\sqrt{47.65} = 32680 \text{ MPa} \quad \text{(A-17)}$$

Ratio of applied stress to strength at time of loading $\sigma/f_{ct0} = 6/47.65 = 0.126$. Because this is less than 0.5, then the nonlinear load factor $R_{LL} = 1$. Time factors $K = 0.25$ days^{-1} and $\beta_{cr} =$ 0.01 days. Other creep compliance parameters are as follows:

$$p_v = 12.5 \times 10^{-6}(f_{cm})^{-0.7} = 12.5 \times 10^{-6}(48)^{-0.7} = 8.32 \times 10^{-7} \text{ MPa}^{-1} \quad \text{(A-18)}$$

$$p_f = 30.0 \times 10^{-6}(f_{cm})^{-0.5} = 30.0 \times 10^{-6}(48)^{-0.5} = 4.33 \times 10^{-6} \text{ MPa}^{-1} \quad \text{(A-19)}$$

$$p_d = 0.023(f_{cm})^{-0.9}(1-g)^{1.7} = 0.023(48)^{-0.9}(1-0.6686)^{1.7} = 1.08 \times 10^{-4} \text{ MPa}^{-1} \quad \text{(A-20)}$$

These parameters are used to compute the compliance function $J(t_T, t_{0T})$, creep coefficient ϕ, and the load-induced strain. Detailed calculations are shown for $t = 365$ days, and the rest of the times are summarized in Table A-2.

Basic creep compliance:

$$p_v\left(1+\frac{1}{Kt_{0T}}\right)=8.32\times10^{-7}\left(1+\frac{1}{0.25*25.43}\right)=9.63\times10^{-7}\ \text{MPa}^{-1} \tag{A-21}$$

$$p_f-\frac{p_v}{Kt_0}=4.33\times10^{-6}-\frac{8.32\times10^{-7}}{0.25*25.43}=4.20\times10^{-6}\ \text{MPa}^{-1} \tag{A-22}$$

$$\begin{aligned}J_b\left(t,t_0\right)&=p_v\left(1+\frac{1}{Kt_0}\right)\ln\left(\frac{t-t_0}{\beta_{cr}}+1\right)+\left(p_f-\frac{p_v}{Kt_0}\right)\ln\left(\frac{t}{t_0}\right)\\&=9.63\times10^{-7}\ln\left(\frac{422.4-25.43}{0.01}+1\right)+4.20\times10^{-6}\ln\left(\frac{422.4}{25.43}\right)=22.0\times10^{-6}\ \text{MPa}^{-1}\end{aligned} \tag{A-23}$$

Drying creep compliance:

$$J_d\left(t,t_0\right)=p_d\left[\Delta H\left(t\right)-\Delta H\left(t_0\right)\right]=1.08\times10^{-4}\left[0.321-0.146\right]=18.8\times10^{-6}\ \text{MPa}^{-1} \tag{A-24}$$

Total compliance:

$$\begin{aligned}J\left(t,t_0\right)&=R_{LL}\left[\frac{1}{E_{ct0}}+R_TJ_b\left(t,t_0\right)+J_d\left(t,t_0\right)\right]\\&=\left(1\right)\left[\frac{1}{32680}+\left(1.154\right)\left(22.0\times10^{-6}\right)+\left(18.8\times10^{-6}\right)\right]=74.8\times10^{-6}\ \text{MPa}^{-1}\end{aligned} \tag{A-25}$$

$$\phi\left(t_T,t_{0T}\right)=E_{ct0}J\left(t_T,t_{0T}\right)-1=32680*74.8\times10^{-6}-1=1.445 \tag{A-26}$$

$$\sigma J\left(t_T,t_{0T}\right)=-6*74.8\times10^{-6}=-449\times10^{-6} \tag{A-27}$$

Table A-2: Results of Creep Calculations

t **(days)**	t_T **(days)**	***J*** **(MPa^{-1})**	**ϕ**	**σJ**	**ε_{sh}**	**ε_{total}**
7	9.277	0	0	0	–36 x 10^{-6}	–36 x 10^{-6}
21	25.43	0	0	0	–258 x 10^{-6}	–258 x 10^{-6}
21.01	25.44	31.5 x 10^{-6}	0.028	–189 x 10^{-6}	–258 x 10^{-6}	–447 x 10^{-6}
365	422.4	74.8 x 10^{-6}	1.445	–449 x 10^{-6}	–566 x 10^{-6}	–1015 x 10^{-6}
10,000	11,540	101 x 10^{-6}	2.290	–604 x 10^{-6}	–666 x 10^{-6}	–1270 x 10^{-6}

Appendix B: Example Calculations for English Units

A 4.0-in. diameter cylinder is cured for t_c = 7 days at T_{cur} = 86°F, after which time it is allowed to dry subjected to T = 77°F and h_0 = 0.70 conditions. The cylinder is later loaded at 21 days with a sustained compressive stress of 870 psi. The design 28-day strength of the cylinder f_c' = 6,000 psi, and it is made from Type I cement. Other mix parameters are unknown.

Compute the time-dependent strains at t = 7 days, 21 days (just before and just after loading), 365 days, and 10,000 days.

Assumed Material Properties

Mean 28-day concrete strength f_{cm} and the aggregate volume fraction g are both unknown, and are therefore estimated from the design strength f_c' = 6,000 psi:

$$f_{cm} = f_c' + 1160 = 6000 + 1160 = 7160 \text{ psi} \tag{B-1}$$

$$g = 0.707 - \frac{f_{cm}}{181300} = 0.707 - \frac{7160}{181300} = 0.6675 \tag{B-2}$$

Temperature Adjustments

Temperature is different from standard conditions, so temperature correction terms must be computed using U = 4500°R:

$$R_c = \exp\left[U\left(\frac{1}{528} - \frac{1}{T_{cur} + 460}\right)\right] = \exp\left[4500\left(\frac{1}{528} - \frac{1}{86 + 460}\right)\right] = 1.324 \tag{B-3}$$

$$R_T = \exp\left[U\left(\frac{1}{528} - \frac{1}{T + 460}\right)\right] = \exp\left[2500\left(\frac{1}{528} - \frac{1}{77 + 460}\right)\right] = 1.154 \tag{B-4}$$

These factors are used to adjust the curing time, time of loading, and analysis times:

$$t_{cT} = R_c t_c = 1.324(7) = 9.271 \text{ days} \tag{B-5}$$

$$t_{0T} = t_{cT} + R_T\left(t_0 - t_c\right) = 9.271 + 1.154(21 - 7) = 25.42 \text{ days} \tag{B-6}$$

$$t_T = t_{cT} + R_T\left(t - t_c\right) = 9.271 + 1.154\left(\begin{bmatrix}365\\10000\end{bmatrix} - 7\right) = \begin{bmatrix}422.2\\11537\end{bmatrix}\text{ days} \tag{B-7}$$

Shrinkage Calculations

The shrinkage coefficient p_{sh} is given by:

$$p_{sh} = 0.963\left(f_{cm}\right)^{-0.5}\left(1-g\right)^{1.7} = 0.963\left(7160\right)^{-0.5}\left(1-0.6675\right)^{1.7} = 0.00175 \tag{B-8}$$

For self-desiccation, parameters p_{au} and β_{au} are given by:

$$p_{au} = 0.012 + \frac{f_{cm}}{725000} = 0.012 + \frac{7160}{725000} = 0.0219 \tag{B-9}$$

$$\beta_{au} = 10^{\left(300\left(f_{cm}\right)^{-0.5}-4\right)} = 10^{\left(300\left(7160\right)^{-0.5}-4\right)} = 5.34\text{ days} \tag{B-10}$$

The volume-to-surface ratio of a cylinder, assuming that the ends are not exposed to drying, is the area of a circle divided by the circumference of a circle, which equals half the radius. Therefore, a 4.0-in. diameter cylinder has V/S = 1.0 in. Being a cylinder with sealed ends, shape factor k_s = 1.18 per Equation (9). These are used to compute the shrinkage half-time τ_{dry}:

$$\tau_{dry} = 51.6\left(k_s\frac{V}{S}\right)^2 = 51.6\left(1.18*1\right)^2 = 71.85\text{ days} \tag{B-11}$$

The change in pore relative humidity ΔH and resulting shrinkage strains ε_{sh} are computed at times t = 7, 21, 365, and 10,000 days. Detailed calculations are shown for t = 365 days, and the rest of the times are summarized in Table B-1.

$$\Delta H_{au}\left(t_T\right) = p_{au}\ln\left(\frac{t_T - t_v}{\beta_{au}} + 1\right) = 0.0218\ln\left(\frac{422.2-0.25}{5.34} + 1\right) = 0.096 \tag{B-12}$$

$$\begin{aligned}\Delta H_{dry}\left(t_T, t_{cT}\right) &= 0.5\left(1-h_0^{\,2}\right)\tanh\left(\sqrt{\frac{t_T - t_{cT}}{\tau_{dry}}}\right)\\ &= 0.5\left(1-0.7^2\right)\tanh\left(\sqrt{\frac{422.2-9.271}{71.85}}\right) = 0.251\end{aligned} \tag{B-13}$$

$$\Delta H(t_T) = \Delta H_{au}(t_T) + \Delta H_{dry}(t_T, t_{cT}) - \Delta H_{au}(t_T)\Delta H_{dry}(t_T, t_{cT})$$
$$= 0.096 + 0.251 - 0.096 * 0.251 = 0.323 \qquad \text{(B-14)}$$

$$\varepsilon_{sh}(t) = -p_{sh}\Delta H(t) = -0.00175 * 0.323 = -565 \times 10^{-6} \qquad \text{(B-15)}$$

Table B-1: Results of Shrinkage Calculations

***t* (days)**	**t_T (days)**	**ΔH_{au}**	**ΔH_{dry}**	**ΔH**	**ε_{sh}**
7	9.271	0.022	0	0.022	-38×10^{-6}
21	25.42	0.038	0.113	0.146	-256×10^{-6}
365	422.2	0.096	0.251	0.323	-565×10^{-6}
10,000	11,536	0.168	0.255	0.380	-666×10^{-6}

Creep Calculations

First, the strength and modulus must be calculated at the time of loading. For Type I cement, a = 4 and b = 0.85, so the strength at t_0 = 21 days (t_{0T} = 25.42 days) is

$$f_{ct0} = f_{cm}\left(\frac{t_{0T}}{a + bt_{0T}}\right) = 7160\left(\frac{25.42}{4 + 0.85 * 25.42}\right) = 7108 \text{ psi} \qquad \text{(B-16)}$$

$$E_{ct0} = 57000\sqrt{f_{ct0}} = 57000\sqrt{7108} = 4823000 \text{ psi} \qquad \text{(B-17)}$$

Ratio of applied stress to strength at time of loading σ/f_{ct0} = 870/7108 = 0.122. Because this is less than 0.5, then the nonlinear load factor R_{LL} = 1. Time factors K = 0.25 days^{-1} and β_{cr} = 0.01 days. Other creep compliance parameters are as follows:

$$p_v = 2.81 \times 10^{-6}(f_{cm})^{-0.7} = 2.81 \times 10^{-6}(7160)^{-0.7} = 5.63 \times 10^{-9} \text{ psi}^{-1} \qquad \text{(B-18)}$$

$$p_f = 2.50 \times 10^{-6}(f_{cm})^{-0.5} = 2.50 \times 10^{-6}(7160)^{-0.5} = 2.95 \times 10^{-8} \text{ psi}^{-1} \qquad \text{(B-19)}$$

$$p_d = 0.014(f_{cm})^{-0.9}(1-g)^{1.7} = 0.014(7160)^{-0.9}(1-0.6675)^{1.7} = 7.31 \times 10^{-7} \text{ psi}^{-1} \qquad \text{(B-20)}$$

These parameters are used to compute the compliance function $J(t_T, t_{0T})$, creep coefficient ϕ, and the load-induced strain. Detailed calculations are shown for t = 365 days, and the rest of the times are summarized in Table B-2.

Basic creep compliance:

$$p_v\left(1+\frac{1}{Kt_{0T}}\right)=5.63\times10^{-9}\left(1+\frac{1}{0.25*25.42}\right)=6.51\times10^{-9}\ \text{psi}^{-1} \tag{B-21}$$

$$p_f-\frac{p_v}{Kt_0}=2.95\times10^{-8}-\frac{5.63\times10^{-9}}{0.25*25.42}=2.87\times10^{-8}\ \text{psi}^{-1} \tag{B-22}$$

$$\begin{aligned}J_b\left(t,t_0\right)&=p_v\left(1+\frac{1}{Kt_0}\right)\ln\left(\frac{t-t_0}{\beta_{cr}}+1\right)+\left(p_f-\frac{p_v}{Kt_0}\right)\ln\left(\frac{t}{t_0}\right)\\&=6.51\times10^{-9}\ln\left(\frac{422.2-25.42}{0.01}+1\right)+2.87\times10^{-8}\ln\left(\frac{422.2}{25.42}\right)=1.49\times10^{-7}\ \text{psi}^{-1}\end{aligned} \tag{B-23}$$

Drying creep compliance:

$$J_d\left(t,t_0\right)=p_d\left[\Delta H(t)-\Delta H\left(t_0\right)\right]=7.31\times10^{-7}\left[0.323-0.147\right]=1.29\times10^{-7}\ \text{psi}^{-1} \tag{B-24}$$

Total compliance:

$$\begin{aligned}J\left(t,t_0\right)&=R_{LL}\left[\frac{1}{E_{ct0}}+R_TJ_b\left(t,t_0\right)+J_d\left(t,t_0\right)\right]\\&=R_{LL}\left[\frac{1}{4823000}+\left(1.154\right)\left(1.49\times10^{-7}\right)+\left(1.27\times10^{-7}\right)\right]=5.09\times10^{-7}\ \text{psi}^{-1}\end{aligned} \tag{B-25}$$

$$\phi\left(t_T,t_{0T}\right)=E_{ct0}J\left(t_T,t_{0T}\right)-1=4823000*5.09\times10^{-7}-1=1.447 \tag{B-26}$$

$$\sigma J\left(t_T,t_{0T}\right)=-870*5.09\times10^{-7}=-443\times10^{-6} \tag{B-27}$$

Table B-2: Results of Creep Calculations

***t* (days)**	**t_T (days)**	**J (psi^{-1})**	**ϕ**	**σJ**	**ε_{sh}**	**ε_{total}**
7	9.277	0	0	0	-38×10^{-6}	-38×10^{-6}
21	25.42	0	0	0	-256×10^{-6}	-256×10^{-6}
21.01	25.43	2.14×10^{-7}	0.028	-186×10^{-6}	-256×10^{-6}	-443×10^{-6}
365	422.2	5.09×10^{-7}	1.447	-443×10^{-6}	-565×10^{-6}	-1008×10^{-6}
10,000	11,536	6.86×10^{-7}	2.296	-597×10^{-6}	-666×10^{-6}	-1262×10^{-6}

A New Way to Predict Creep and Shrinkage

An ACI Foundation-funded research project

by Victoria K. Sicaras, on behalf of the ACI Foundation

Having creep and shrinkage modeling tools to accurately predict concrete behavior over time is essential for designing and maintaining serviceable, safe structures. Knowing how long a structure's useful service life should be, and how concrete performs under sustained loads, is instrumental in determining when retrofits are needed or whether structural issues are materializing. This is particularly important for creep-sensitive structures, such as high-rise buildings, concrete box-girder bridges, and prestressed beams. However, many time-dependent models are outdated with respect to today's growing database of experimental evidence. A new research study funded by the ACI Foundation aims to rectify this issue.

Emerging from the research is a time-dependent design model that captures the complex reality of how creep and shrinkage phenomena are interconnected. Using solidification theory, the researchers calibrated the new model to meet the twin objectives of simplicity in application and theoretical rigor. It is poised for adoption into ACI design guidelines regarding creep and shrinkage, prestress losses, and deflections of concrete structures.

The Need for New Models

ACI Committee 209, Creep and Shrinkage in Concrete, reports information on creep and shrinkage of concrete and concrete structures. Documents published by the committee include ACI PRC-209.2-08, Guide for Modeling and Calculating Shrinkage and Creep in Hardened Concrete[1]; ACI PRC-209.1-05, Report on Factors Affecting Shrinkage and Creep of Hardened Concrete[2]; and ACI PRC-209-92, Prediction of Creep, Shrinkage, and Temperature Effects in Concrete Structures (Reapproved 2008).[3]

Since their initial publication in the 1990s through the early 2000s, the guides have relied on a creep and shrinkage model developed in 1982 to calculate time-dependent deformations. In 2019, however, ACI Committee 209 determined that the model no longer reflected the current understanding of time-dependent behavior and discontinued support for that model. Experimental evidence collected over the past few decades indicated the model may no longer perform well for long-term (multi-decade) creep and shrinkage predictions, and especially for large or complex structures.

"At the time when the provisions were developed, that model reflected the best knowledge that we had about creep and shrinkage. But when you start to apply it to modern design practices with modern mixtures, beyond how it was originally intended, it breaks down and doesn't work properly," explained Brock Hedegaard, Principal Investigator of the research project and Secretary of ACI Committee 209.

To ensure ACI Committee 209 guidelines align with modern practices and structures, a new model was needed to reflect advances in knowledge about creep and shrinkage mechanisms. In 2019, Hedegaard began working with committee member—and now committee Chair—Mija Hubler on a research proposal with the goal of bringing to life such a model. They found a champion for their work in the ACI Foundation's Concrete Research Council (CRC).

Each year, CRC hosts a request for proposals (RFP) program that awards funding to several concrete research projects. Hedegaard and Hubler's RFP was selected to receive funding in 2020.

Getting Funded

The proposal involved calibrating a creep and shrinkage model that uniquely facilitates both traditional integral-type and modern rate-type analyses (refer to textbox). To create and calibrate the model, researchers needed to curate and vet a comprehensive database, which was a challenging task in itself, Hedegaard said. They also had to identify the appropriate input parameters and perform statistical comparisons to select the final model.

"This sort of undertaking would have been extremely difficult to get off the ground without the ACI Foundation and CRC," Hedegaard stated. "What we were doing did not really qualify as basic research, because we were working with already established databases and not adding new data, and there aren't a lot of funding entities interested in that. But bringing things up to date and making design documents applicable to the state of practice is incredibly valuable."

ACI Foundation Executive Director Ann Masek agreed: "ACI technical committees regularly need updates to their technical work product, and we were pleased with the opportunity to support this critical research need of ACI 209."

CRC's open RFP program allows researchers to submit unsolicited research projects. A major requirement is that the research must be endorsed by at least one ACI technical committee. Thanks to funding from ACI and donations to research from the ACI community, the number of grants awarded has grown significantly over the last several years. The funding is awarded based on relevancy and potential impact of the research, overall proposal quality, researcher capability, supplemental support for the project (such as collaboration with other funders and organizations), and ACI technical committee engagement. In the case of the time-dependent model project, it had unanimous endorsement by ACI Committee 209, as well as commitments from several of the industry's leading design and engineering companies to serve on an advisory panel.

"Not only will the research results advance industry practice, with its updated model prediction of time-dependent deflections and stresses in concrete structures, but we also got a chance to support the work of early career professors like Brock [Hedegaard] and Mija [Hubler]," Masek said.

Project Details

Name: Calibration of Simplified Creep and Shrinkage Models Developed Using Solidification Theory

Principal Investigator: Brock Hedegaard, Associate Professor of civil engineering at the University of Minnesota, Duluth, MN

Co-Principal Investigator: Mija Hubler, Associate Professor and the Co-Director of the Center for Infrastructure, Energy and Space Testing at the University of Colorado, Boulder, CO

ACI Technical Committee endorsement: ACI Committee 209, Creep and Shrinkage in Concrete

Funder: ACI Foundation's Concrete Research Council

About the Research: Traditional time-dependent analysis has relied on definition of a compliance function or creep coefficient. For time-varying stresses, the strain may be approximated (for example, through the age-adjusted modulus method) or computed using integral-type analysis. Rate-type analysis does not require computation of an integral over the entire stress history; thus, it is more efficient and accurate for more complex structural analysis. Previously, no existing time-dependent model other than the B3/B4 basic creep expression had a convenient form for performing rate-type analysis.

The model developed over the course of this research project changes this reality. The new model has closed-form expressions for the compliance function and compliance rate, uniquely supporting both analysis approaches. These features place the model on the cutting edge of time-dependent structural analysis.

The calibration was conducted in three steps:

1. Database management and preparation;
2. Identification of appropriate input parameters and calibration by nonlinear optimization; and
3. Statistical comparison and final model selection per information theory.

Supporting Early Career Faculty

At the time of funding, Hedegaard was an Assistant Professor of civil engineering at the University of Minnesota, Duluth, MN, USA. Hubler, who served as Co-Principal Investigator on the project, was an Assistant Professor of civil, environmental, and architectural engineering at the University of Colorado, Boulder, CO, USA. One graduate research assistant contributed to the research.

The ACI Foundation shares ACI's vision of a future where everyone has the knowledge needed to use concrete effectively to meet the demands of a changing world. To support this shared vision, the Foundation's mission is to make strategic investments in ideas, research, and people to create the future of the concrete industry.

"Investing in 'people' is a critical component of the mission, and it drives CRC's efforts to award at least two grants annually to projects led by an associate or assistant professor or other type of early career faculty," according to CRC Chair Sulapha Peethamparan. "This helps us make sure we are aiding the promotion and development of future generations of concrete researchers."

The grants also limit funding of research organizations' indirect costs to 15%. This ensures the funds are directed to the people and activities involved in a project and not the organization's overhead.

"Receiving the funding needed to conduct research helps young professionals like us contribute to academia and industry, and those research projects are great bullet points to have when seeking tenure," Hedegaard said. "But also, most of the CRC grant money we received was used to fund our student's tuition and other project-related needs. Our student was important to the project because he helped develop the model, plus he was doing all the number crunching and MATLAB work."

Mutual Benefits of Industry Involvement

"Our industry advisory panel was very helpful in terms of brainstorming model candidates," Hedegaard said. "We had building engineers, bridge engineers, and a distribution of people who had performed creep and shrinkage testing."

The project's advisory panel included representatives from FIGG Bridge Group; Meyer Borgman Johnson (MBJ); MJ2 Consulting; Skidmore, Owings & Merrill (SOM); Wiss, Janney, Elstner Associates (WJE); and WSP USA. Ongoing dialogue between the researchers and panel members guided the concept of a model that incorporates the interconnectedness of creep and shrinkage.

"MJ2 Consulting's Matt D'Ambrosia brought up the fact that different types of creep and shrinkage don't occur separately. They are connected in some way because it all comes down to what happens to water in concrete. Factoring in these relationships between creep and shrinkage phenomena is one of the reasons why the model does very well in comparison with the databases. It's a big leap forward for our industry, I hope," Hedegaard explained.

Panel members also provided input on what they would want to see in a design document, which was beneficial for both the researchers and the companies involved, Hedegaard said. Because the model aligns with industry best practices where it makes sense to do so, it is both useful for theoretical predictions and as a practical tool in real-world applications.

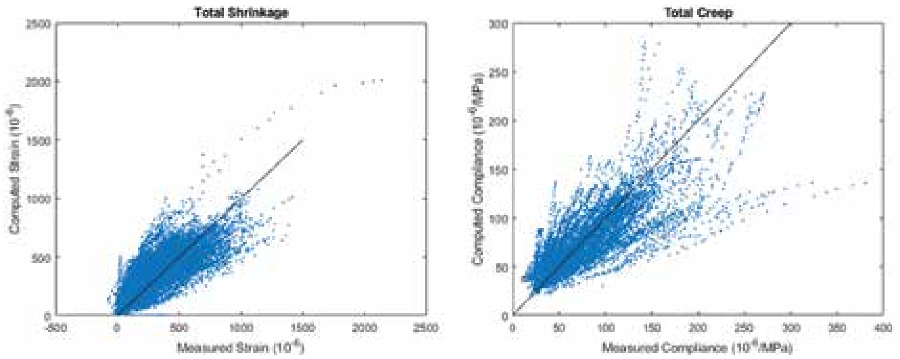

The research project's calibrated model predictions compared to measurements from the Northwestern University creep and shrinkage database (based on Fig. 8 in Reference 4)

Brock Hedegaard checks out a double-ring concrete shrinkage test at the Turner-Fairbank Highway Research Center laboratory in McLean, VA, USA *(photo courtesy of Brock Hedegaard)*

Advancing the Concrete Industry

During the project duration, results were presented at ACI convention Open Topic technical sessions and regular meetings of ACI Committee 209. Roman Wan-Wendner, ACI Subcommittee 209-D Chair and ACI Committee 209 Vice Chair, served as committee liaison between the project team, the advisory panel, and Committee 209.

"The project was a positive and fun process," Hedegaard said. "There was a lot of back and forth as we bounced ideas around, and a lot of creative thinking from multiple angles and parties. What we ended up with was a model that is a very good fit to the database, but it's also a tool that you can take to your design office and use."

A manuscript documenting the calibrated model was published in the May 2023 issue of *ACI Materials Journal*.[4] The model also will be presented to ACI Committee 209 for incorporation into ACI PRC-209.2. In addition, it will be featured in two planned reports from Committee 209 documenting time-dependent structural analysis by either traditional integral methods or modern rate-type methods. The model, which facilitates both, is expected to form the basis for robust design guidance in both documents.

The ACI Foundation looks forward to funding future research and innovations that provide needed solutions for industry needs, Masek said. Organizations can aid the Foundation's efforts and support concrete-related research and technology advancements by contributing their expertise, experience, and donations. Visit **www.acifoundation.org/giving** for more details.

References

1. ACI Committee 209, "Guide for Modeling and Calculating Shrinkage and Creep in Hardened Concrete (ACI PRC-209.2-08)," American Concrete Institute, Farmington Hills, MI, 2008, 45 pp.

2. ACI Committee 209, "Report on Factors Affecting Shrinkage and Creep of Hardened Concrete (ACI PRC-209.1-05)," American Concrete Institute, Farmington Hills, MI, 2005, 12 pp.

3. ACI Committee 209, "Prediction of Creep, Shrinkage, and Temperature Effects in Concrete Structures (ACI PRC-209-92) (Reapproved 2008)," American Concrete Institute, Farmington Hills, MI, 1992, 47 pp.

4. Hedegaard, B.D.; Clement, T.J.; and Hubler, M.H., "Coupled Pore Relative Humidity Model for Concrete Shrinkage and Creep," *ACI Materials Journal*, V. 120, No. 3, May 2023, pp. 103-116.

Selected for reader interest by the editors.

Victoria (Vikki) K. Sicaras is an Account Manager with Advancing Organizational Excellence (AOE), an ACI subsidiary that provides marketing and association management consulting services. She has more than 20 years of experience writing and editing for leading construction industry publishers, with a focus on concrete construction.